FUNCTIONAL CHARACTERIZATION OF TWO PHENYLACETYL-COA LIGASES IN BURKHOLDERIA CENOCEPACIA

By

Ijeme A. Imolorhe

A Thesis submitted to the Faculty of Graduate Studies of

the University of Manitoba

In partial fulfillment of the requirements for the degree of

MASTER OF SCIENCE

Department of Microbiology

University of Manitoba

Winnipeg, Manitoba

Abstract

Burkholderia cenocepacia causes Cepacia syndrome, a fatal pneumonia that affects Cystic Fibrosis patients. Aromatic degradation has been linked to virulence in *B. cenocepacia* by insertional mutagenesis of genes involved in phenylacetic acid catabolism. *B. cenocepacia* has two paralogous copies of PaaK, the phenylacetyl-CoA ligase, which produces PA-CoA, the inducer of the pathway. Our objective was to assess a role for PaaK1 and PaaK2 in PA metabolism and virulence by constructing clean deletion mutants for each gene, and a double *paaK* mutant, as well as to quantify virulence using the nematode host model. Deletion and complementation of *paaK1* revealed no change in killing phenotype. Reporter activity assays revealed PaaK1-dependent induction of the PA pathway by 3-hydroxyphenylacetic acid but not 4-hydroxyphenylacetic acid. Altogether, these results demonstrate that 3-OHPA induces the PA degradation pathway in a *paaK1* dependent manner and that PaaK1 is not involved in pathogenicity.

ACKNOWLEDGEMENTS

I would like to express my deepest gratitude to my project supervisor Dr. Silvia Cardona for the opportunity granted to gain research skills and laboratory experience as well as her invaluable guidance and patience.

I would also like to thank my graduate committee members Dr. Anne Karen Brassinga and Dr. John Sorensen for their recommendations and advice.
Special thanks to Dr. Brassinga for helping with the *C. elegans* protocols.

I would also like to thank the Department of Microbiology, University of Manitoba and the Faculty of Graduate Studies for lending the use of equipment and providing educational and administrative support.

I would like to thank the National Science and Engineering Research Council (NSERC) for providing the funding for this project.

Thanks to April Gislasson, Arbia Arfaoui, Karen LoVetri, Harry Yudistira, Ruhi Bloodworth, Tanya Pribytkova and other past and present members of the Cardona Lab for their friendship and support.

Finally, I would like to express my deepest gratitude to my family, particularly my parents Sam and Stella Imolorhe, for providing emotional support through this process.

Table of Contents

List of Tables

List of Copyrighted Material for which permission has been obtained

Flannagan, R. S., Linn, T., and Valvano, M. A. (2008). A system for the construction of targeted unmarked gene deletions in the genus *Burkholderia*. *Environ. Microbiol.* 10, 1652-1660.

Holden, M. T., Seth-Smith, H. M., Crossman, L. C., Sebaihia, M., Bentley, S. D., Cerdeno-Tarraga, A. M., Thomson, N. R., Bason, N., Quail, M. A., Sharp, S., Cherevach, I., Churcher, C., Goodhead, I., Hauser, H., Holroyd, N., Mungall, K., Scott, P., Walker, D., White, B., Rose, H., Iversen, P., Mil-Homens, D., Rocha, E. P., Fialho, A. M., Baldwin, A., Dowson, C., Barrell, B. G., Govan, J. R., Vandamme, P., Hart, C. A., Mahenthiralingam, E., and Parkhill, J. (2009). The genome of *Burkholderia cenocepacia* J2315, an epidemic pathogen of cystic fibrosis patients. *J. Bacteriol.* 191, 261-277.

Law, A., and Boulanger, M. J. (2011). Defining a Structural and Kinetic Rationale for Paralogous Copies of Phenylacetate-CoA Ligases from the Cystic Fibrosis Pathogen *Burkholderia cenocepacia* J2315. *J. Biol. Chem.* 286, 15577-15585.

Law, R. J. (2009). The Relationship between Phenylacetic acid Catabolism and Pathogenicity of *Burkholderia cenocepacia* K56-2 in the *Caenorhabditis elegans* Host Model.

Luengo, J. M., Garcia, J. L., and Olivera, E. R. (2001). The phenylacetyl-CoA catabolon: a complex catabolic unit with broad biotechnological applications. *Mol. Microbiol.* 39, 1434-1442.

Teufel, R., Mascaraque, V., Ismail, W., Voss, M., Perera, J., Eisenreich, W., Haehnel, W., and Fuchs, G. (2010). Bacterial phenylalanine and phenylacetate catabolic pathway revealed. *Proc. Natl. Acad. Sci. U. S. A.* 107, 14390-14395.

List of Figures

List of Abbreviations

3-OHPA	3-hydroxyphenylacetic acid
4-OHPA	4-hydroxyphenylacetic acid
ACP	Acyl carrier protein
AMP	Adenosine monophosphate
ANL	**A**cyl coa synthtase; **N**onribosomal Peptide synthetase; **L**uciferase
Ara-4-N	4-amino-4-deoxy-L-arabinose
ATP	Adenosine triphosphate
BCC	*Burkholderia cepacia* Complex
BCESM	***B**urkholderia **c**enocepacia* **E**pidemiological **S**train **M**arker
CF	Cystic fibrosis
CFTR	Cystic fibrosis transmembrane conductance regulator
Cm	Chloramphenicol
CoA	Coenzyme A
DDT	Dichlorodiphenyltrichloroethane
ET-12	Edinburgh-Toronto clone 12
Gm	Gentamicin
IL	Interleukin
Km	Kanamycin
L4	Larval stage 4
LB	Luria broth

LPS	Lipopolysaccharide
NGM	Nematode growth media
NRPS	Nonribosomal Peptide synthetase
PA	Phenylacetic acid
PAH	Polyaromatic hydrocarbon
PCB	Poly-chlorinated biphenyls
PCR	Polymerase chain reaction
PPi	Pyrophosphate
RND	Resistance-nodulation-division
rpm	Revolutions per minute
TAE	Tris base, Acetic acid and EDTA
Tc	Tetracycline
Tp	Trimethoprim

1. Introduction

1.1. CF and cepacia syndrome

Cystic Fibrosis is an autosomal recessive, genetic disease that affects multiple organ-systems in the body. It manifests in early infancy, featuring wide ranging symptoms such as pulmonary inflammation, chronic airway infection, pancreatic insufficiency, low weight and nutrient malabsorption. The most common respiratory symptom is the development and non-clearance of thick mucus in the lungs (muscoviscidosis) which interferes with breathing and can only be cleared by violent coughing. It is found predominantly among people of Northern European descent (1 in every 3000 births) with more than 100 times fewer cases in individuals of Asian and African descent (O'Sullivan and Freedman, 2009). Cystic Fibrosis is caused by a mutation in the Cystic Fibrosis Transmembrane Conductance Regulator (CFTR) a chloride channel which serves a variety of other functions such as inhibiting sodium chloride from entering through epithelial sodium channels and facilitating the bicarbonate-chloride exchange (Quinton, 2008). Consequently, CFTR is closely involved in maintaining a balanced environment on the surface of the epithelial cells containing enough moisture to allow regular clearance of mucus containing bacteria and other particles picked up from the air. A non-functional CFTR results in the buildup of a poorly soluble, viscous mucus in the lung comprised of a high concentration of salts and mucins, and amino acids. All of these components provide nutrient-rich media for bacteria such as *Pseudomonas aeruginosa* and *Staphylococcus aureus* which, in a healthy individual, would ordinarily be flushed out by the mucocilliary clearance action of respiratory epithelial cells (O'Sullivan and Freedman, 2009).

Over a thousand mutations in the CFTR have been linked to Cystic Fibrosis. Of these, more than a majority is caused by the absence of a phenylalanine at position 508. This mutation, denoted as F508del (where F=phenylalanine), results in trafficking errors that lead to the nascent

protein being ubiquinated and degraded. Other types of mutations resulting in cystic fibrosis could be due to an early stop codon or defective regulation of the protein (O'Sullivan and Freedman, 2009). As of yet there is no cure for cystic fibrosis.

1.2. Cepacia Syndrome

In the late 1970s and early 1980s, several CF patients presented with bacteremia and sepsis associated with a fatal rapid pulmonary decline. This acute condition was brought on by a respiratory infection caused by bacterial species then known as *Pseudomonas cepacia* later renamed *Burkholderia cepacia* and later shown to be a complex of related species (Isles et al., 1984; Vandamme et al., 1997). The condition called Cepacia Syndrome is easily transmissible from patient to patient and very difficult to treat due to the multidrug resistant nature of *Burkholderia* species. This development necessitated a need for understanding the virulence mechanisms of these species.

1.3. Burkholderia sp., B. cepacia complex (BCC), and Burkholderia cenocepacia

Burkholderia sp. are non-fermenting, obligate aerobic Gram negative rods which occur naturally in the soil and rhizosphere. The *Burkholderia* genus is partly comprised of the *Burkholderia cepacia*,complex (BCC) a grouping of genetically distinct yet phenotypically similar *Burkholderia* strains. The type strain *Burkholderia cepacia* was first identified as the causative agent of sour skin disease in onions by William Burkholder who classified it as *Pseudomonas cepacia* (Burkholder, 1950). It was later distinguished from other Pseudomonads and renamed *Burkholderia* (Yabuuchi et al., 1992) (Vandamme et al., 1997). Seventeen genetically distinguishable species have now been identified and comprise the *Burkholderia*

cepacia complex (BCC). Despite the circumstances in which they were discovered, the BCC have been shown to serve a positive agricultural benefit by providing antifungal protection to crops. They are widely ecologically distributed and have been shown to be hardy, nutritionally versatile. They have the ability to utilize a wide variety of complex substrates including many (e.g. DDT) that are pollutants (Balandreau et al., 2001). Accordingly, BCC strains have been considered as a possible bioremediation tool. The proposed positive applications of the BCC have been eclipsed by their emergence, during the last three decades, as opportunistic pathogens responsible for infections in Cystic Fibrosis and other immune-compromised patients. Of the seventeen BCC species, *B. multivorans* and *B. cenocepacia* are the most commonly linked to hospital acquired infections and Cepacia Syndrome in CF patients, and are the most studied in the area of virulence and pathogenicity.

1.4. Burkholderia cenocepacia natural niche

Burkholderia species are ubiquitous in nature. They are found in such wide-ranging environment as soil, sea water, various plant rhizospheres worldwide and more recently in hospitals (see above). *Burkholderia* species occupy multiple ecological niches and various symbiotic relationships with plants, fungi and insects. Although, they are largely non-pathogenic, some species are known to be phytopathogenic in various plant species. A few examples are *Burkholderia plantarii,* which causes blight in rice crops, and *B. caryophili,* which causes plant wilt. They have been isolated from many fungal species with which they associate as endo-symbionts and may even assist fungal phytopathogenicity by secreting toxins (Compant et al., 2008; Lim et al., 2003). Some species have similar relationships with insects. *Burkholderia sp.* have an interesting triangular symbiotic relationship with a plant, and an insect documented by

Santos *et al.* Some *Burkholderia sp.* are endosymbionts of *Atta sexdens rubrilpilosa* ants which build and nest in fungal gardens of *Leucoagaricus gongolophorus*. The bacteria secrete a mycotoxin that kills all fungal species except the particular one symbiotic to the insect. Similarly, these species produce antifungal toxins that protect plant roots in the rhizosphere (Santos et al., 2004). *Burkholderia* species adapt to different environments by assuming and exploiting different roles.

1.5. Genome of B. cenocepacia K56-2

B. cenocepacia strain K56-2 descends from the ET-12 (Edinburgh-Toronto clone 12) lineage isolates from cross-Atlantic epidemic of cepacia syndrome in the late 1980s that affected patients in Canada and the United Kingdom. It is clonally related to the sequenced strain J2315.

B. cenocepacia K56-2 has a large genome of 8.06 Mbps composed of three chromosomes (Figure 1). Chromosome 1 is the largest chromosome with 3.87 Mbps compared to the medium-sized Chromosome 2 which has 3.22 Mbps. Chromosome 3 is the smallest chromosome at 0.8 Mbps. Finally, the genome also includes a plasmid which consists of at 0.092Mbps of DNA (Holden et al., 2009). Chromosome 1 consists of genes involved in core cell functions such as metabolism and division whereas chromosomes 2 and 3 consist of genes that have protective function or originate from horizontal gene transfer (Holden et al., 2009). The size of the genome gives the strain the genetic and metabolic versatility which allows easier adaptation to different or difficult environments and available nutrients.

Fig. 1. ***B. cenocepacia* J2315 Genome** consists of (A) a large chromosome (BCAL-3.87 Mbps), (B) a medium chromosome (BCAM-3.22Mbps) and (C) small chromosome (BCAS-0.8Mbps) and (D) a plasmid (pJ2315-0.098) (Holden et al., 2009)

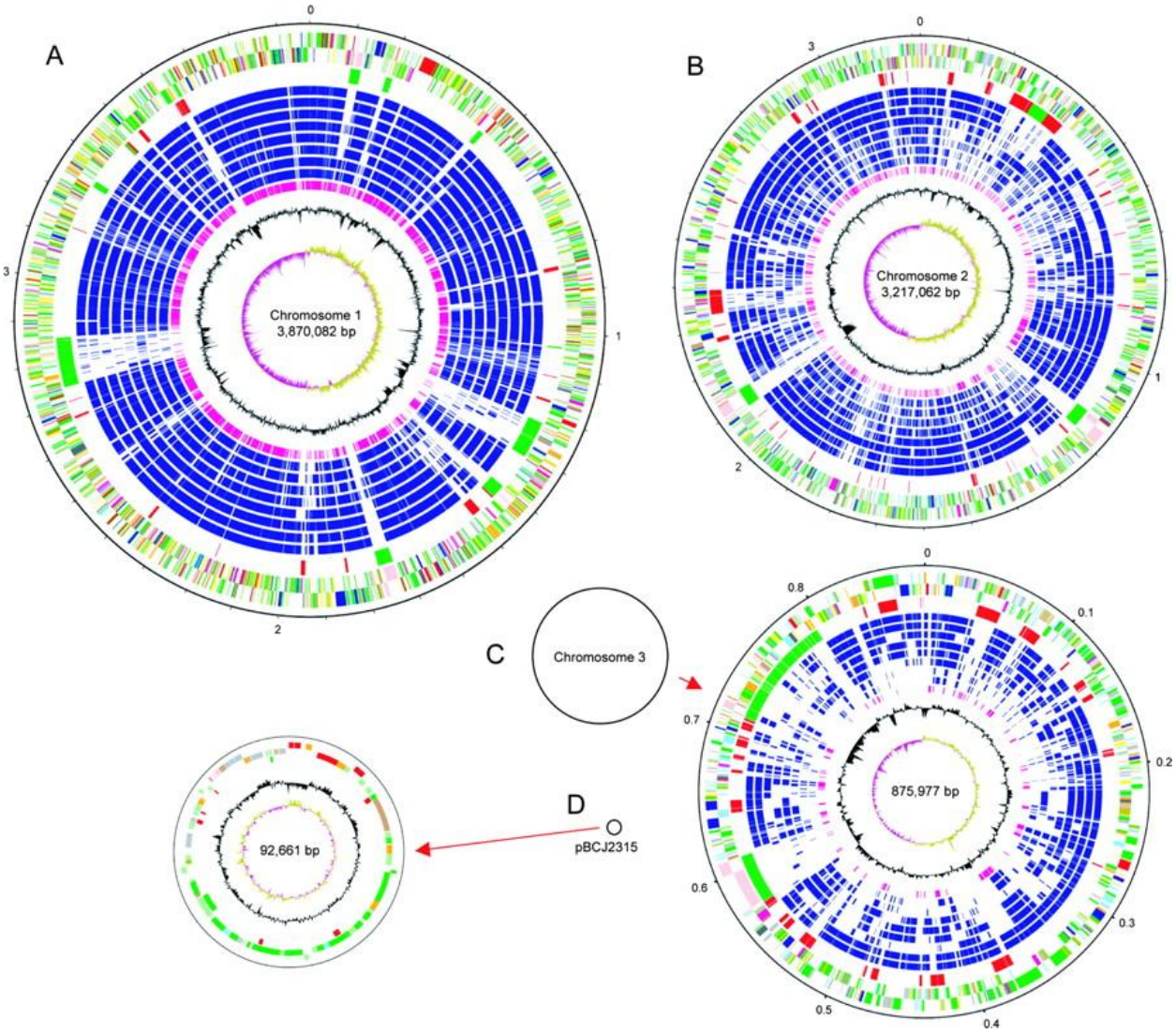
A
Chromosome 1
3,870,082 bp
B
Chromosome 2
3,217,062 bp
C
Chromosome 3
875,977 bp
D
pBCJ2315
92,661 bp

1.6. Virulence Factors in B. cenocepacia

B. cenocepacia is notoriously difficult to counter with conventional antibiotic means, and is known for its ability to evade host defenses in the CF lung. Its persistence is believed to be partly due to its remarkable ability to adapt to diverse environments by engaging several virulence determinants to establish infections. These are some of the major virulence factors found in *B. cenocepacia*:

1.6.1. Antibiotic Resistance

B. cenocepacia, a multi-drug resistant bacterium, has several mechanisms to counter the effects of antibiotics. Like many Gram-negative bacteria, *B. cenocepacia* employs the use of multi-drug efflux pumps as a primary defense against antibiotics. Resistance-Nodulation-Division (RND) is a major style of drug efflux utilized wherein three proteins, a cytoplasmic membrane transporter, a perisplamic adaptor protein and an outer-membrane channel protein, complex to transport drugs out of the cell. *B. cenocepacia* has as many as 16 RND efflux systems and least two (RND-3 and RND-4) have been demonstrated to contribute significantly to antibiotic resistance (Bazzini et al., 2011). Additionally, RND proteins have been linked to secretory functions like the secretion of acyl homoserine lactones in association with quorum sensing as well as secretion of siderophores for iron acquisition (Drevinek and Mahenthiralingam, 2010).

1.6.2. Host Defence Evasion

In the CF lung, *B. cenocepacia* persists by evading host defences in a number of ways. *B. cenocepacia* is able to survive macrophages engulfment by preventing cell maturation and

phagolysosomal fusion with Bcc-containing vacuoles in a process associated with alternate sigma factor RpoE. This allows time for the bacteria to activate genes that are involved in resistance. *B. cenocepacia* is also able to impede the activities of other immune cells such as neutrophils and dendritic cells (Saldias and Valvano, 2009). Another well known mechanism is the use of zinc metallo-proteases which mainly function to degrade structural tissue proteins such as collagen, and fibronectin (Mahenthiralingam et al., 2008). *B. cenocepacia* has two broad spectrum zinc metalloproteases ZmpA and ZmpB that also degrade antimicrobial peptides which have been linked to bacterial survival. The two genes appear unrelated even though they have same function (Kooi and Sokol, 2009).

1.6.3. Biofilm formation

As an opportunistic colonizer of the CF lung, *B. cenocepacia* creates biofilms for protection from antibiotics and host immune responses, as well as facilitates chemical signalling and quorum sensing. *B. cenocepacia* has a complex quorum sensing mechanism mediated by proteins *cepR* and *cepI*. The *cepIR* system mediates the secretion of ***N***-octanoylhomoserine lactone which allows cell-to-cell communication and coordinated gene expression and plays a role in drug resistance (Peeters et al., 2008). In the CF lung environment, the *cepIR* quorum sensing system has been shown to be involved in inter-specific communication with *Pseudomonas aeruginosa* (Loutet and Valvano, 2010; Tomlin et al., 2001). The *cepIR* system regulates many other processes related to the virulence including secretion of siderophores and has been linked to virulence using the nematode host model (Kothe et al., 2003) . A second quorum sensing system *ccir* controls many of the same process but appears to have a reverse regulatory relationship with the *cepIR* system (Malott et al., 2009).

1.6.4. Siderophores

Siderophores are secreted compounds that chelate soluble iron Fe^{3+} ions in the environment after which they are recognized then reintroduced back into the cell. RND efflux pumps are believed to play a role in the secretion of siderophores. This ensures that the iron supply to the cell is not limited. Bcc strains produce four distinct siderophores (Darling et al., 1998)(Loutet and Valvano, 2010). Of those, the major siderophore produced in *B. cenocepacia* is ornibactin which has been linked to virulence using the nematode and rat agar bead infection models. In addition to the activity of the siderophores, *B. cenocepacia* exploits the characteristic concentration of ferritin in the CF lung as a source of soluble iron.

1.6.5. BCESM Pathogenicity

The ***B****urkholderia* ***c****enocepacia* ***E***pidemiological ***S***train ***M***arker (BCESM) is part of the *cci* pathogenicity island unique to *B. cenocepacia* among Cepacia syndrome causing Bcc species. It is identifiable by RAPD fingerprinting and was used in the reclassification of *B. cenocepacia* from *B. cepacia* genomovar III. It harbours putative virulence genes such as the *ccir* quorum sensing system and an amidase and a porin as well as some genes involved in metabolic activity; an major premise for the assertion that metabolic processes are linked to pathogenicity in *B. cenocepacia* (Baldwin et al., 2004) (Loutet and Valvano, 2010).

1.6.6. Motility and Adherence

Motility is important in an infection for bacterial dissemination from the entry site to other host organs. As with the rest of the Bcc, *B. cenocepacia* strains have a single polar flagellum that enables swimming and the spread of infection. Aside from their primary purpose,

flagella (and their constitutive proteins flagellins) have been linked to virulence in *B. cenocepacia* due to their facilitating the invasion of epithelial cells by coordinating adherence. Flagellins also induce an inflammatory response in the host when they are recognized by Toll-like receptors and this initiates a cascade that culminates in the production of cytokines such as IL-8 (interleukin-8) which causes respiratory decline by causing tissue damage. Flagellar proteins are also involved with other virulence factors such as biofilm formation and type 3 and type 4 secretion systems (Tomich M et al., 2002; Urban TA et al., 2004). Interruption of the flagellin gene *fliC* results in an attenuated pathogenicity phenotype. A key structure in adherence is the cable pilus, unique to the ET-12 lineage strains among the Bcc. Cable pili are fimbriae associated with a 22 KDa adhesin that bind to cytokeratin 13 a filamentous protein that is found on the surface of respiratory epithelial cells. This step allows the bacteria to breach and kill the epithelial cell (Urban et al., 2005).

1.6.7. Lipopolysaccharide (LPS) layer

As with other gram negative bacteria, the LPS of *B. cenocepacia* is an important virulence determinant. *Burkholderia* species have constitutive expression of 4-amino-4-deoxy-L-arabinose (Ara-4-N) in the inner core of the LPS unlike other bacteria which only express this residue *in vivo*. The core O antigen portion of the LPS prevents the cell from being engulfed by macrophages or binding to epithelial cells. The core oligosaccharide has been shown to be necessary for virulence *in vivo,* and necessary for survival in macrophages (Loutet and Valvano, 2010).

1.6.8. Metabolism

B. cenocepacia is a hardy organism due to its arsenal of metabolic operons that allow survival and persistence in hostile environments. It stands to reason that some of these processes have links to virulence in host organisms or competing bacteria based on the findings showing that they are globally controlled by some interrelated factors. One example is the acyl carrier protein (ACP) which is a key player in fatty acid biosynthesis. ACPs donate the acyl moiety to activate two CoA molecules to condense to form a fatty acid chain. This process results in the creation of important glycolipids, endotoxins and signaling molecules involved in growth and pathogenesis. Without ACP, *B. cenocepacia* expresses an attenuated killing phenotype in the *Caenorhabditis elegans* model (Sousa et al., 2011). Similarly, the phenazine biosynthesis regulator (Pbr) has been linked to virulence in *B. cenocepacia*. The Pbr regulates the production of phenazines, heterocyclic nitrogenous compounds which are also antimicrobial. It is also a pleiotropic regulator of growth, aromatic amino acid synthesis, stress resistance and virulence. The importance of the Pbr is evidenced by a *pbr* deletion mutant which does not grow in minimal media and has an attenuated pathogenicity in *C. elegans* killing assays (Ramos et al., 2010). Finally, the phenylacetic acid degradative pathway has been linked to pathogenicity in wildtype isolate K56-2, by reports that insertional mutagenesis attenuates (*paaA* and *paaE*) or enhances (*paaF* and *paaZ*) pathogenicity (Law et al., 2008) (Hunt et al., 2004).

1.7. Aromatic Catabolism and Biodegradation

The major source of naturally occurring aromatic compounds is lignin which occurs interstitially in the plant cell wall. Lignin comprises 25% of the Earth's biomass and is primarily broken down by microbes. The most common compound resulting from this breakdown is

benzene (Diaz et al., 2001). Aromatic degradation features across many bacterial genera. Known examples include *Acinetobacter*, *Alcaligenes*, *Burkholderia*, and *Pseudomonas* in particular which is the most extensively studied (Cao et al., 2009). Aromatics degrading bacteria are metabolically diverse and able to live in multiple ecological niches. As a case in point, *Escherichia coli* strains live in the soil, where they degrade aromatic compounds related to plant decomposition. Concomitantly, they degrade amino acids that result from the breakdown of short peptides by proteases and peptidases in the gut (Diaz et al., 2001).

In general, aromatic biodegradation involves peripheral pathways that converge at a central activated intermediate which is then degraded to common compounds. Aromatic biodegradation occurs via aerobic and anaerobic pathways depending on the bacterial species and ecology. Anaerobic biodegradation relies on chemotrophic reduction using nitrates, carbon (IV) oxide, iron or sulfates as electron acceptors (Cao et al., 2009). Benzoyl-CoA, the central molecule of the anaerobic aromatic degradation pathway, results from activation of benzoate (resulting from the breakdown of phenylalanine) by the benzoyl-coA ligase. Following activation, the ring is de-aromatized by the action of a benzoyl-coA reduction and a series of β-oxidation steps result in Acetyl-CoA. Aerobic degradation utilizes oxygen as an electron acceptor and an activator. Typically, the ring is oxygenated by mono-oxygenases and/or dioxygenases to yield dihydroxyl-substituted aromatics such as homoprotecatechuate, catechol, gentisate, protocatechuate, homoprotocatechuate, and homogentisate. The ring is then cleaved via *ortho* (in between the –OH groups) or *meta* cleavage (next to the distal OH group) (Díaz, 2004). Finally, the resulting chain is metabolized into Kreb's intermediates. The phenylacetic acid pathway is termed an aerobic hybrid pathway because it combines the early activation of the aromatic molecule by thioesterification found in the anaerobic pathways with the oxygenation

and ring cleavage featured in the aerobic pathways (Diaz et al., 2001). It is the central pathway that is utilized in the breakdown of styrene, 2-phenylethylamine, trans-styrylacetic acid, phenylacetaldehyde, phenylacetic acid, phenylacetylamides, phenylacetyl esters and n-phenylalkanoic acids with an even number of carbon atoms (Luengo et al., 2001). The degradation of aromatic compounds is a delicate dance among the relevant gene clusters. For instance in *E. coli* (and other aromatics-degrading bacteria) the *mao* (mono-amine oxidase) cluster catalyses the denitrification of 2-phenylethylamine to phenylacetaldehyde. Another gene *padA* (**p**henyl**a**cetaldehyde **d**ehydrogenase; called *feaB* in *B. cenocepacia*) downstream of the *paa* cluster produces the protein that oxidizes phenylacetaldehyde to phenylacetic acid which is then activated by PaaK to PA-CoA which induces the rest of the PA degradative pathway (Diaz et al., 2001).

The foremost significance of microbial aromatic biodegradation is its possible application as a tool for bioremediation. In the last century, human activity has introduced xenobiotic pollutants into the environment. Xenobiotic compounds include mono- and polycyclic chlorinated aromatic as with poly-aromatic hydrocarbons (PAHs) and poly-chlorinated bi-phenyls or PCBs (that are released due to activities relating to industry and manufacturing), nitro-substituted aromatic compounds, pesticides (DDT), or mixtures of aromatic compounds such as BTEX (benzene, toluene, ethyl benzene and xylene) which result from the burning of fossil fuels. Besides polluting the environment, many of these compounds pose significant health risks (Lu et al., 2011). More than half of the problematic xenobiotics are halogenated compounds (Zhang and Bennett , 2005). This is a major problem because chlorine, from PCBs, has an electron withdrawing ability and a larger size that interferes with the activity of oxygenases preventing breakdown of the compound. As a result, one particular mechanism that has been

extensively studied is reductive dehalogenation, which entails the removal of halogen substituents from the ring structure using dehalogenases. Dehalogenation involves replacing the chlorine atom with an OH (hydrolytic dehalogenation), an oxygen atom (via an oxygen dependent pathway) or a hydrogen atom (reductive halogenation). Reductive halogenation is generally found in anaerobes in which it is more thermodynamically favorable and convenient because it is requires no oxygen and has a better application to the remediation of groundwater contamination (Cao et al., 2009; Copley, 1997).

Many bacteria are able to degrade naturally occurring compounds with similar molecular structures to the xenobiotic compounds and some microbes in contaminated sites adapt to using the pollutants as carbon sources. Consequently, certain species are being studied along these lines as their metabolic machinery can be applied to degrading xenobiotics. For instance, *Pseudomonas putida* is known for its ability to degrade toluene while *B. xenovorans* LB400 is able to degrade PCBs (as is *B. cepacia*) (Cao et al., 2009; Field and Sierra-Alvarez, 2008; Goris et al., 2004).

1.8. The PA pathway and the paa operon

The phenylacetic acid PA pathway is the central pathway through which upper aerobic degradative pathways from complex aromatic compounds converge at phenylacetate-CoA (PA-CoA) which can be degraded to TCA intermediates acetyl-CoA and succinyl-CoA (Figure 2). This system is well distributed among bacteria and fungi (Figure 3). The PA pathway is significant for including a classic anaerobic step, activation with Coenzyme A, in an otherwise aerobic pathway. Via the classical aerobic pathway, found in fungi, phenylacetic acid is broken down to fumarate and acetoacetate through the homogentisate pathway which involves

oxygenolytic ring cleavage. For this reason, the PA pathway is generally referred to as a hybrid in terms of oxygen use and availability (Mingot et al., 1999; Teufel et al., 2010).

Fig. 2. **The Phenylacetyl-CoA Catabolon.** Degradative Pathways of different aromatic compounds (styrene, 2-phenylethylamine, trans-styrylacetic acid, phenylacetaldehyde, phenylacetic acid, phenylacetyl amides, phenylacetyl esters and n-phenylalkanoic acids containing an even number of carbon atoms) converge at phenylacetyl-CoA. (Luengo et al., 2001)

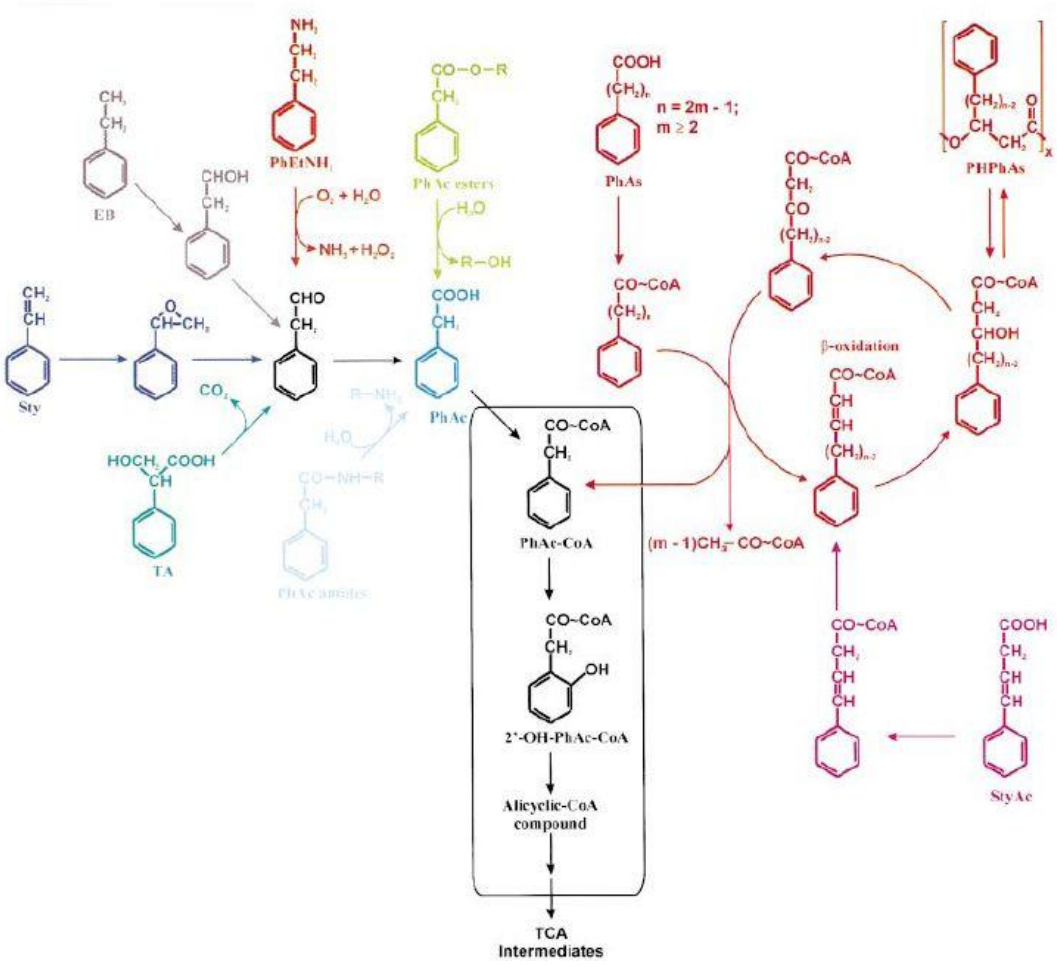
EB
PhEtNH2
PhAc ester
PhAs
n = 2m - 1;
m ≥ 2
PHPhAs
Sty
PhAc
TA
PhAc amides
β-oxidation
PhAc-CoA
2'-OH-PhAc-CoA
Alicyclic-CoA compound
TCA Intermediates
(m - 1)CH3- CO~CoA
StyAc

Fig. 3. **Organization of the *paa* operons of different bacterial species.** (Luengo et al., 2001)

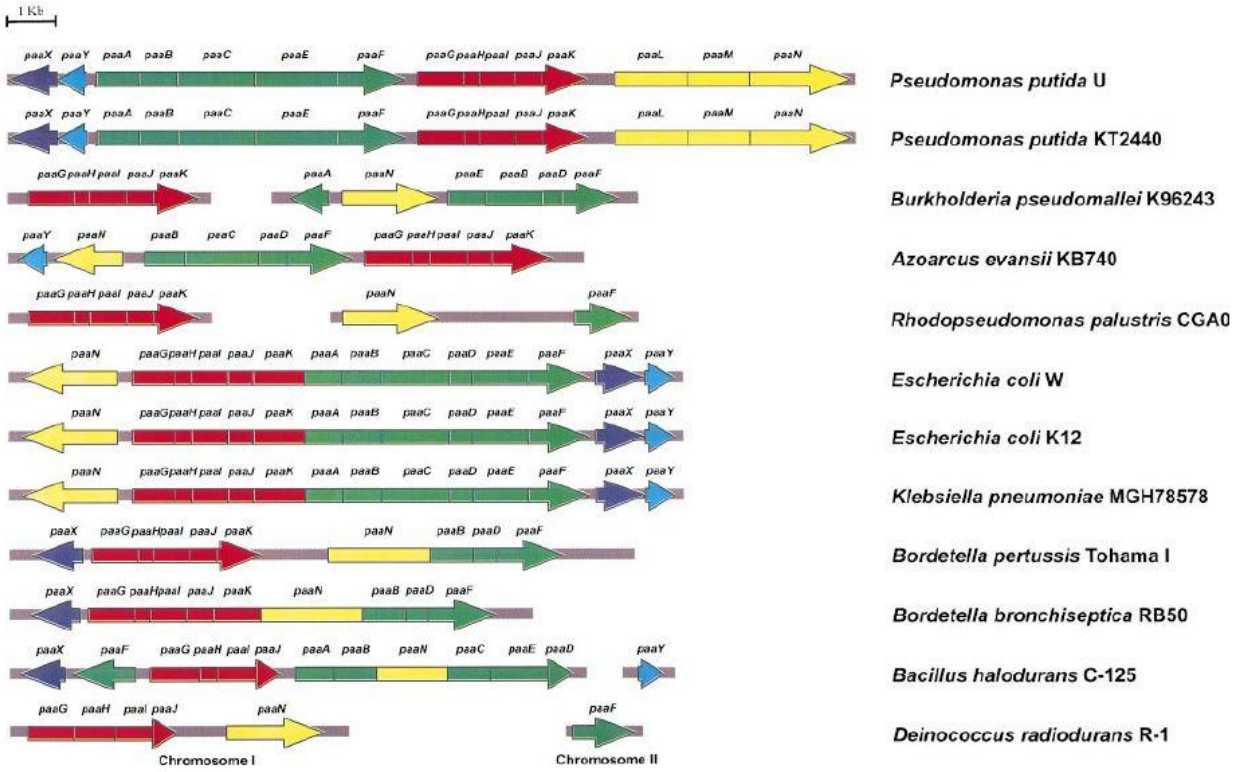
1 Kb
paaX paaY paaA paaB paaC paaE paaF paaG paaH paaI paaJ paaK paaL paaM paaN
Pseudomonas putida U
Pseudomonas putida KT2440
Burkholderia pseudomallei K96243
Azoarcus evansii KB740
Rhodopseudomonas palustris CGA0
Escherichia coli W
Escherichia coli K12
Klebsiella pneumoniae MGH78578
Bordetella pertussis Tohama I
Bordetella bronchiseptica RB50
Bacillus halodurans C-125
Deinococcus radiodurans R-1
Chromosome I
Chromosome II

In *E. coli*, the enzymes of the PA pathway are encoded by a 14 gene operon in three transcriptional units *paaXY, paaZ, paaABCDEFGHIJK* (Figure 4). In comparison, the *B. cenocepacia paa* operon is organized in 3 sections (Figure 5) *paaABCDE* and *paaFZJGIK1* on chromosome 1 and *paaHK2* on chromosome 2. The steps of the full pathway were recently elucidated for *E. coli* K12 and *Pseudomonas putida* Y2 (Teufel et al., 2010) and are shown in Figure 6. PA is first ligated to CoA by the phenylacetate-CoA ligase PaaK (El-Said Mohamed, 2000; Martinez-Blanco et al., 1990b). The Coenzyme A thioester of PA is then oxidized to a 1,2-epoxy PA-CoA by a monoxygenase complex of PaaABCDE enzymes (Teufel et al., 2010). The epoxide is isomerized to the ring-expanded oxepin by PaaG, which is in turn transformed to 2,3-dehydroadipyl-CoA in a series of ring-opening and oxidation steps, where PaaZ cleaves the ring in the presence of PaaG, producing a highly reactive aldehyde that is oxidized to 3-oxo-5,6-dehydrosuberyl-CoA (Teufel et al., 2011), PaaJ transforms the resulting ß-keto C_8 intermediate to 2,3-dehydroadipyl-CoA and PaaF catalyzes the subsequent conversion of the C_6 intermediate to 3-hydroxyadipyl-CoA (Teufel et al., 2010). The PA degradative pathway is subject to catabolite repression in the presence of sugar based carbon sources such as glucose (Martinez-Blanco et al., 1990a).

1.9. The Phenylacetyl CoA ligase

PaaK, the phenyl acetyl-CoA ligase, catalyses the formation of PA-CoA, the common carbon intermediate linking the upper and lower degradative pathways in the aerobic degradation of aromatic compounds as demonstrated in *E. coli* and *Pseudomonas* spp. (Ferrandez et al., 1998; Martinez-Blanco et al., 1990b; Vitovski, 1993). The formation of PA-CoA is the first step of the *paa* pathway and is a key step as PA-CoA is the inducer of the pathway (Garcia et al., 2000). As

the catalyst of the first step of the PA degradative pathway, PaaK serves an important role in inducing the pathway by producing PA-CoA. The enzyme itself is expressed and induced by the presence of phenylacetic acid (or its hydroxyl-derivatives). PaaK is also involved in producing PA-CoA as a side-chain precursor to penicillin G (benzylpenicillin) in fungi *Penicillium chrysogenum* (Mingot et al., 1999) (Rodriguez-Saiz M et al., 2001) (Miñambres et al., 1996).

Fig. 4. ***E. coli* K12 *paa* operon** consists of 14 genes and three transcriptional units *paaZ, paaABCDEFGHIJK* and *paaXY*. *E. coli* has one *paaK* (PA-CoA ligase) (Teufel et al., 2010)

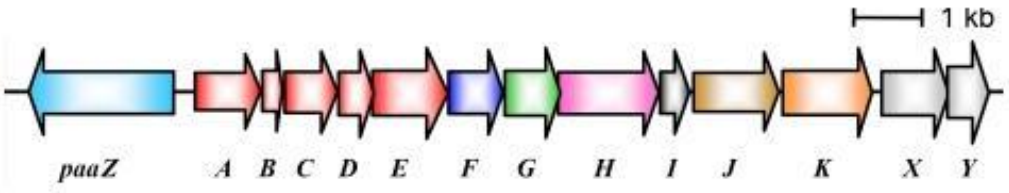
1 kb
paaZ
A
B
C
D
E
F
G
H
I
J
K
X
Y

Fig. 5. ***Burkholderia cenocepacia paa* operon** showing the three transcriptional units *paaABCDE*, *paaFZJGIK1* and *paaHK2*. (Imolorhe and and Cardona, 2011)

Note that *paaG* on the second chromosome is a predicted gene function for BCAM1710.

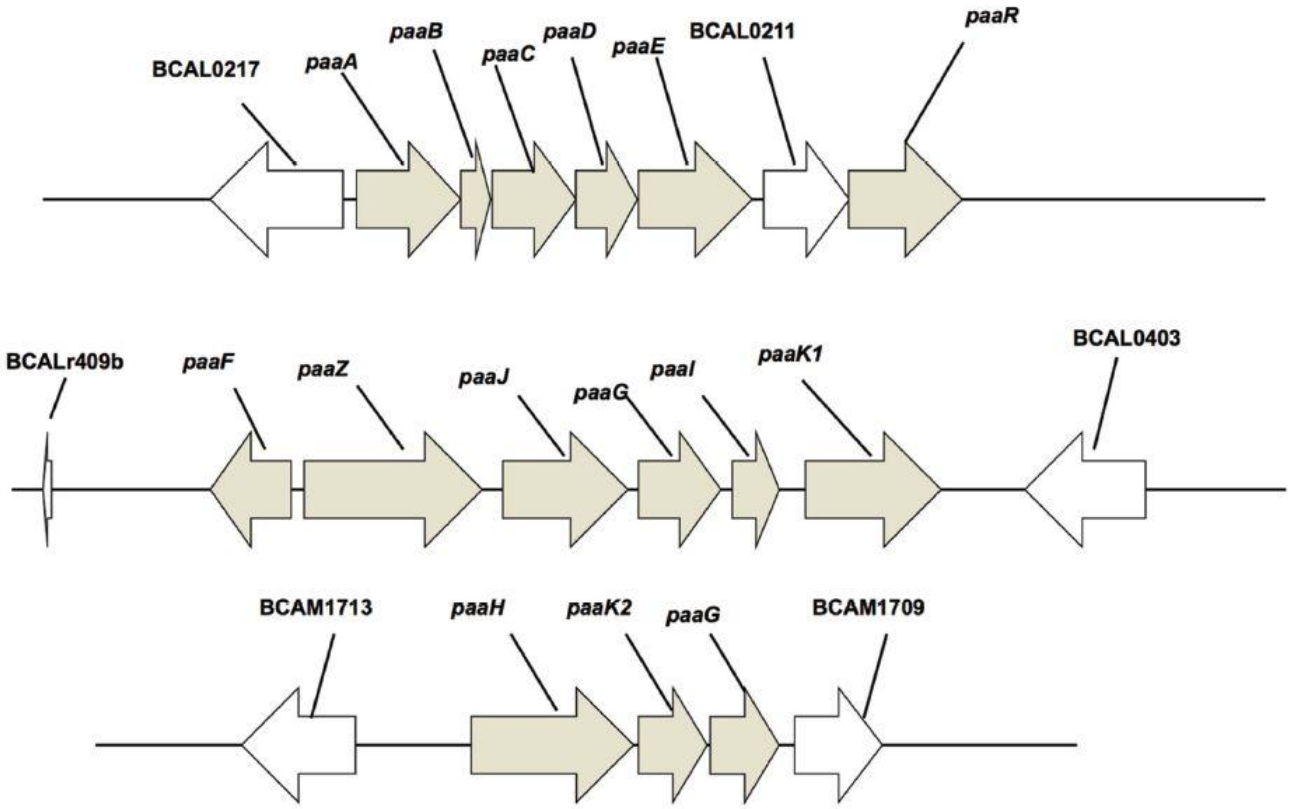
BCAL0217
paaA
paaB
paaC
paaD
paaE
BCAL0211
paaR
BCALr409b
paaF
paaZ
paaJ
paaG
paaI
paaK1
BCAL0403
BCAM1713
paaH
paaK2
paaG
BCAM1709

Fig. 6. **The phenylacetic acid degradative pathway** elucidated for *E. coli* K12 and *Pseudomonas* strain Y2 (Teufel et al., 2010)

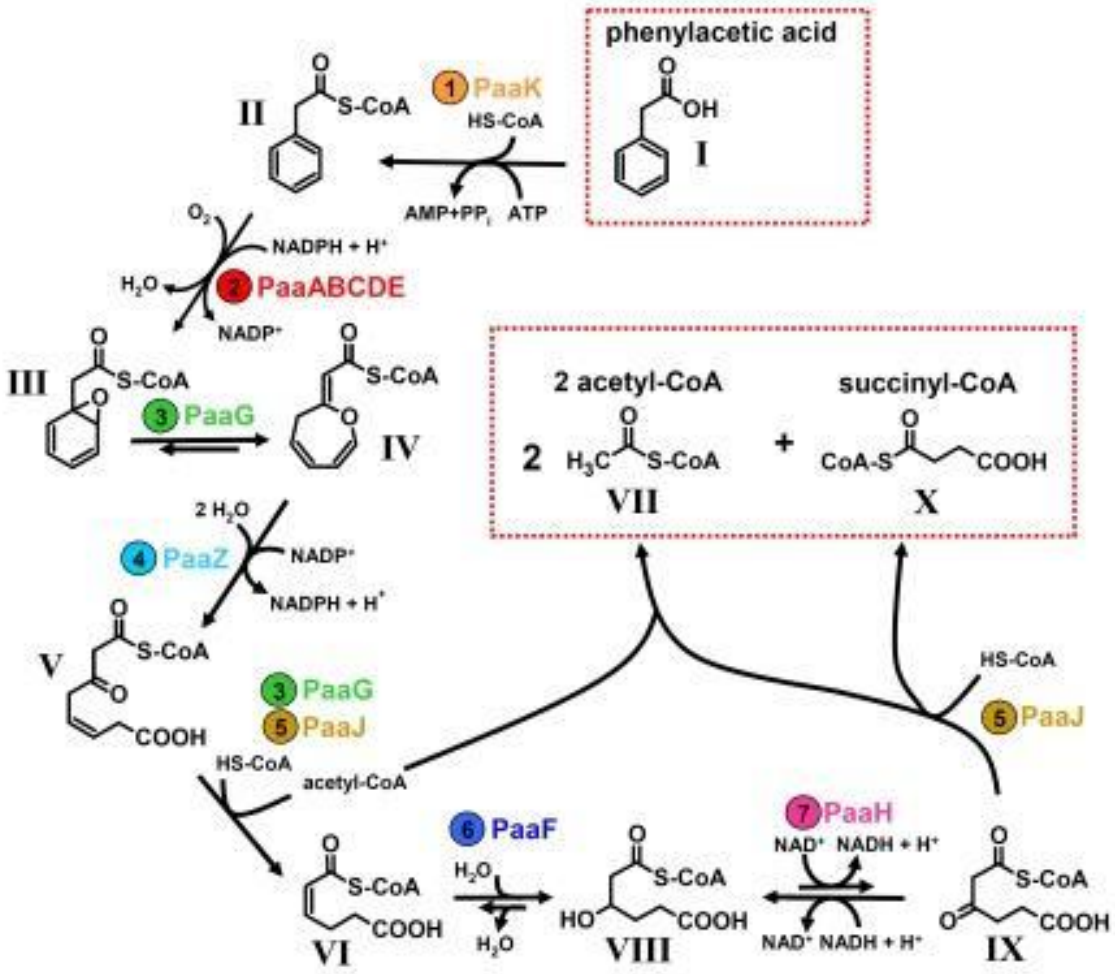
phenylacetic acid
I
II
1 PaaK
HS-CoA
AMP+PP$_i$ ATP
O_2
NADPH + H$^+$
H_2O
2 PaaABCDE
NADP$^+$
III
3 PaaG
IV
2 acetyl-CoA
2
VII
succinyl-CoA
+
X
2 H_2O
4 PaaZ
NADP$^+$
NADPH + H$^+$
V
3 PaaG
5 PaaJ
HS-CoA
acetyl-CoA
HS-CoA
5 PaaJ
6 PaaF
H_2O
H_2O
VI
VIII
7 PaaH
NAD$^+$ NADH + H$^+$
NAD$^+$ NADH + H$^+$
IX

1.10. The ANL superfamily

The PA-CoA ligase, PaaK , belongs to the ANL family of adenylate-forming enzymes. The ANL super family is comprised of three subgroups of the Adenylate Forming Enzymes; the **A**cyl-and aryl CoA synthetases (ligases), **N**on-ribosomal Protein Synthetases (NRPS) adenylation domains and **L**uciferase enzymes. PaaK belongs to the acyl/aryl CoA synthetase subfamily. These enzymes are grouped together because they catalyze a common two-step reaction. The conserved first step consists of the transfer of an adenylate (AMP) molecule, resulting from the cleavage of an ATP (Adenosine tri-phosphate) molecule and the release of a pyrophosphate (PPi), to a carboxylate functional group. A magnesium ion coordinates the reactive pyrophosphate leaving group. The first step activates the substrate molecule for a second step which for the acyl-coA synthtases involves a thiol group attacking the carboxylate carbon and displacing the AMP (Gulick, 2009; Schmelz and Naismith, 2009). The general reaction proceeds as follows:

E + MgATP + R-COOH →[E-R-CO-AMP] + MgPPi

[E-R-CO-AMP] + CoASH → R-CO-SCoA + E + AMP + PPi + H_2O.

(Villemur, 1995)

ANL superfamily enzymes have distinguishing structural hallmarks; specifically, two α/β domains, a large N-terminal domain and a smaller C-terminal domain. Crystal structures of an acetyl Co-A synthetase from *Salmonella enterica* reveal two conformations for the common sites corresponding to the two steps of the adenylation-thioesterification step found in acyl-CoA synthetases and demonstrate that the two reactions are catalyzed by the same enzyme adopting 2 sequential conformations (Gulick et al., 2004).

1.11. Why does B. cenocepacia have twoPA-CoA ligases?

Unlike *E. coli*, *B. cenocepacia* has two genes which encode a PA-CoA ligase. *paaK1*, is located on chromosome 1 and *paaK2*, is located on chromosome 2. They are not identical proteins a with 69% similarity. Additionally, *paaK1* is a structurally a dimer, whereas *paaK2* is a monomer. Despite this, both ligases appear to serve the same function i.e. activation of PA as insertional mutation or deletion of *paaK1* does not result in a growth defective phenotype in the presence of PA as a sole carbon source (Law et al., 2008). It is not unusual for an organism to have more than one PA-CoA ligase. An example is marine bacteria *Desulfobacterium autotrophicum* which also has two ligases (Uniprot.org). *Pseudomonas sp.*Y2 has two *paa* gene clusters *paa1* and *paa2* that are similar to each other with each having a ligase denoted *paaF* and *paaF3* respectively (del Peso-Santos et al., 2008). A third ligase *paaF2* with its own promoter is located just upstream of the *paa1* gene cluster and is flanked on the upstream side by regulatory genes for the styrene degradative upper pathway. Expression of *paaF2* is believed to be under the control of the *sty* regulator gene as it is only induced in the presence of styrene. It is possible that the reason *B. cenocepacia* has two PA-CoA ligases might be that they be differentially up-regulated by upper pathway substrates. A recent article by Law and Boulanger shows differences between *paaK1*and *paaK2* in the Km (Michaelis Constant) and thus overall binding affinity for PA and hydroxylated PA molecules 3-OHPA and 4-OHPA (Law and Boulanger, 2011). Along these lines, one of the major premises of this work is that *paaK1* and *paaK2* can be differentiated based on their preferred substrates.

Table 1. General Differences Between PaaK1 and PaaK2

General Differences Between PaaK1 and PaaK2	
PaaK1	**PaaK2**
BCAL0404 (Chromosome 1)	BCAM1711 (Chromosome 2)
Dimer	Monomer
Larger substrate binding pocket	Smaller substrate binding pocket
Native protein	Horizontal gene transfer

1.12. Burkholderia cenocepacia Host Models

B. cenocepacia expresses virulence in a various organisms. Before its emergence as an opportunistic human pathogen it was discovered and studied as a plant pathogen in onions and has been used to study alfalfa seedlings (Balandreau et al., 2001; Burkholder, 1950). Virulence in this strain is more commonly studied in the animal model in which it is evidenced across phyla. The most common model is the rat/mouse agar bead model which was repurposed from studies with *Pseudomonas aeruginosa* and is useful for setting up long term infections of *B. cenocepacia* although without presentation of CF symptoms. Mice defective for the CFTR are slightly better for producing phenotypes similar to human CF symptoms (Valvano et al., 2005). Studies have also been conducted using non-mammals like zebra-fish and invertebrates like the wax moth *Galleria mellonella* and nematode *Caenorhabditis elegans*(Loutet and Valvano, 2010). The latter two tend to be cheaper and less time consuming to maintain and are gaining popularity in use (Cardona et al., 2005).

1.13. C. elegans as a Host Model

Caenorhabditis elegans is a soil dwelling, free living, nematode round worm that feeds on bacteria. They are 1mm in length and transparent, which allows easy viewing under the microscope. They are largely hermaphrodites with males occurring every 0.05% of the population. Under standard lab conditions, one self-fertilizing hermaphrodite can lay up to 100-300 eggs. The entire life cycle from egg to adult stages is about 4 days and they are easily maintained on nematode growth media (NGM) inoculated with *E .coli* OP50, a uracil autotroph at 15 ^{o}C. Under these conditions, the worms survive for as long as two weeks (Aballay and Ausubel, 2002) . They are easily manipulated genetically via DNA microinjection. The temporal

and financial cost as well as the relative ease of propagating and maintaining *C. elegans* strains relative to mammalian hosts makes them a preferred host .*C. elegans* is well-known as a model organism in research because it is one of a few metazoans with an entirely sequenced genome. Similar to many nematodes, *C. elegans* display eutely, a constant number of somatic cells through adulthood as such each stem cell can be traced to its differentiated form. They have 40% genome homology with humans and are susceptible to infection and killing by some bacteria that are human pathogens such as *Staphylocccus aureus* . Additionally, *C. elegans* have a rudimentary innate system and no discernible adaptive immune system, making this species amenable as a host organism for infection assays with opportunistic bacteria such as *Burkholderia* sp. (Aballay and Ausubel, 2002; Kurz and Ewbank, 2003). Accordingly, *C. elegans* is an excellent tool for understanding disease and bacterial pathogenesis.

2. Hypothesis

The phenylacetic acid degradative pathway plays a role in the virulence mechanisms of *Burkholderia cenocepacia*. PaaK as the activator of the pathway inducer PA-CoA is central to the PA pathway. *Burkholderia cenocepacia* has 2 genes that encode a PA-CoA ligase. The two ligases PaaK1 and PaaK2 can be characterized and differentiated based on substrate and biochemistry and may play different roles in the pathogenicity of *B. cenocepacia*.

3. Materials and Methods

3.1. Bacteria Strains, Nematode Strains and Growth conditions

All bacterial strains were stored in LB glycerol stocks at -80^{o}C. All liquid overnight bacterial cultures were grown in LB at 37 ^{o}C with shaking at 210 rpm. *E. coli* overnight cultures were supplemented with 20µg/ml tetracycline, 50µg/ml gentamicin (Gm), 40µg/ml kanamycin (Kan), 20µg/ml chloramphenicol (Cm) and 50µg/ml trimethoprim (Tp) as needed. *B. cenocepacia* overnight culture media were supplemented with 100µg/ml tetracycline, 50µg/ml gentamicin, and 100µg/ml trimethoprim as needed. Nematode strains were obtained from the Caenorhabditis Genetics Centre and were maintained according to protocols prescribed by the CGC Worm Stocks were propagated every 5 days at 15^{o}C (Stiernagle, 1999).

Table 2: Strains and Plasmids

Strain or Plasmid	Features	Reference or source
***E. coli* strains**		
DH5α	F-_Φ80 *lacZΔ* M15 *endA1 recA1 hsdR17*(r_K-m_K+) *supE44 thi-1Δ gyrA96 (ΔlacZYAarg-F)U169 relA1*	Invitrogen
SY327	Z-Competent cells	(Miller and Mekalanos, 1988)
MM290	Helper strain	(Izard et al., 1992)
W14	Spontaneous *paa* operon mutant	(Ferrandez et al., 1998)
***B. cenocepacia* strains**		
K56-2	ET12 clone related to J2315, CF clinical isolate	
RJL1	K56-2Δ*paak1*,	(Law, 2009)
IAI1	K56-2Δ*paak1*	This Study
STC179	K56-2::pGPomegaTp paaA, Tp^r	(Law et al., 2008)
STC155	K56-2::pGPomegaTp paaE, Tp^r	(Law et al., 2008)
Plasmids		
pAAD	*E. coli paa* operon	
pAADTn1000-46	*E. coli paa* operon with Tn-1000-46 interrupting *paaK*	
pDA12	DHFR promoter, Tc^r	(Aubert et al., 2008)
pDA12*paaK1*	DHFR promoter with *B. cenocepacia* paaK1, Tc^r	Boulanger Lab
pDA12*paaK2*	DHFR promoter with *B. cenocepacia* paaK2, Tc^r	Boulanger Lab
pDAI-*Sce*I	DHFR promoter controlling e-ISce-I, Tc^r	(Flannagan et al., 2008)
pGPI-*Sce*I	DHFR, ISceI recognition sequence, Tp^r	(Flannagan et al., 2008)
pJH1	dhfr promoter controlling eGFP, Cm^r	(Hamlin et al., 2009)
pJH2	eGFP –no start codon, Cm^r	(Hamlin et al., 2009)
pJH6	paaZ promoter controlling eGFP, Cm^r	(Hamlin et al., 2009)
pJH7	paaA promoter controlling eGFP, Cm^r	(Hamlin et al., 2009)
pJH8	paaH promoter controlling eGFP, Cm^r	(Hamlin et al., 2009)
pRK2013	Helper plasmid, Kan^r	(Figurski and Helinski, 1979)
pRL5	DHFR, ISceI recognition sequence; paaK1 flanking regions, Tp^r	(Law et al., 2008)
pRL7	DHFR, ISceI recognition sequence; paaK2 flanking regions, Tp^r	(Law, 2009)

Cm, chloramphenicol; Gm, Gentamicin; Kan, Kanamycin; Tc, Tetracycline; Tp, Trimethoprim

3.2. Bacterial Growth

Bacterial cultures were grown overnight in LB with appropriate antibiotics. They were washed, resuspended in a 400µL (unless otherwise noted) of Phosphate Buffer Saline (PBS) and inoculated into a 5ml test tube M9 minimal media with the innoculum being the number of cells in a 100µL volume at an OD600nm of 2.

3.3. Nematode Slow Killing Assays

Caenorhabditis elegans strain DH26 worms were used as the model organism because they are temperature sensitive and can be sterilised by incubating the eggs at 25^{o}C thereby allowing for ease of counting. Thirty to forty sterile L4 larvae were allowed to graze on bacterial lawns on modified nematode growth media (30% more peptone) for seven days at 25^{o}C and live worms were counted daily for the duration. Kaplan Meier curves were generated from the data using GraphPad Prism 5. Statistical significance was determined as a P value that is less than 0.05 using the Log-rank test (Law et al., 2008).

3.4. Synchronization of L4 larvae

Six to ten DH26 adults were transferred to two 35mm NGM plates spotted with 50mL of an *E. coli* OP50 culture at an OD of 1.7 and incubated for 7 days at 15^{o}C until the plate was loaded with eggs. Worms and eggs were washed off the plates with sterile distilled water to a final collected volume of about 5 ml. The worm/egg wash liquid was treated with a mixture of 0.6ml water, 0.5ml 10-13% sodium hypochlorite and 0.4ml 5N sodium hydroxide and vortexed every two minutes for 6 minutes. The mixture was then separated into four 1.5ml micro-

centrifuge tubes and spun down at 3500 rpms for 30s. The pellets were washed twice with sterile water combined, and finally re-suspended in 200ml of water. A sample of the suspension was checked for the presence of eggs in a microscope. The suspension was spotted on fresh NGM+ *E. coli* OP50 and incubated for 2 days until hatchlings developed into L4 larvae.

3.5. Molecular Biology Techniques

All modifications to *B. cenocepacia* strains were carried out using triparental mating (Craig et al., 1989). The *paaK1* deletion mutant was created by triparental mating; by introducing the previously created plasmid pRL5 with helper plasmid pRK2013 (Figurski and Helinski, 1979) and wild type *B. cenocepacia* strain K56-2 as the recipient. Relevant plasmids were stored in competent *E. coli* DH5α or SY327 cells. Competent cells for *E. coli* strains DH5α, W14, W14pAAD, and W14pAAD Tn-1000-46 (See Table 2) were prepared using cold calcium chloride (Cohen et al., 1972). *E. coli* SY327 competent cells were prepared using the Z-Competent™ *E. coli* Transformation Kit protocol. Plasmids were introduced into *E. coli* strains by heat shock at 42^0 C. Resulting transformants were selected using the relevant antibiotic on solid LB media and then screened by colony PCR using primers specific to the plasmid (Table 3).

3.6. E. coli/ paaK Complementation with B. cenocepacia paaK genes

Competent *E. coli* W14pAAD-Tn1000-46 cells were transformed with pDA12*paaK1* or pDA12*paaK2* (provided by M. Boulanger). Transformation was confirmed by antibiotic selection and colony PCR for the presence of the plasmid and insert. The complemented strain

(*E. coli* W14pAAD-Tn1000-46/pDA12*paak1* and *E. coli* W14pAAD-Tn1000-46pDA12*paaK2*), the background strain (*E. coli* W14pAAD-Tn1000-46) and a wild-type like strain *E. coli* W14pAAD were grown in M63 minimal media plus 5mM PA or 0.1 % glycerol. Media was supplemented with of 1µg/ml vitamin B1 and 5ng/ml B12 as well as 0.01mM $CaCl_2$. Strains were grown at 30^{o}C for 24 hours with shaking (210rpms). Readings were taken on a Biotek 2 plate reader.

3.7. Tri-parental mating with B. cenocepacia

100µL of a *B. cenocepacia* K56-2 overnight culture was inoculated into a fresh 5ml LB broth tube and allowed to grow for three hours into early log phase at an OD of between 0.3 and 0.6. Concomitant to the original inoculation of K56-2 the previous day, *E. coli* pRK2013 and the *E. coli* strain harboring the donor plasmid were streaked out on solid SOB media with the relevant antibiotic (Kan for the *E. coli* pRK2013). Donor and Helper strain lawns were collected into 5mL volumes of PBS and mixed and OD600nm readings were taken, and, based on these readings, expected volumes were calculated for 0.5 ml suspension at an OD600nm of 1 for the recipient (K56-2) and 1.5 ml at an OD of 0.3 for the donor and helper. The three volumes were combined, spun down and re-suspended in 100µL SOC broth and then spotted in the middle of a SOB plate. The spot was allowed to grow lid side up overnight and was collected into 2mL of LB and re-suspended. 100µL -200µL of suspension was spread on LB agar with gentamicin and the selective antibiotic specific to the donor plasmid. 10^0 and 10^{-1} dilutions were spread. For triparental matings involving the mutagenesis plasmid pDAI-*Sce*I only 10^0 dilutions were used.

3.8. Colony PCR Screening

Isolated colonies were streaked out on LB agar plus relevant selective antibiotic and incubated overnight at 37^{o}C. Cell suspensions were made by touching a 200uL plastic pipette tip to a flame, allowing it to cool and then collecting a little material from the plate and re-suspending the material in 100uL of sterile water. For each sample, 2µL of cell suspension was added to a PCR mix of 4.3 µL sterile water, 0.2µL of a 10mM solution of deoxynucleotides triphosphates, 0.2µL each of forward and reverse primers (100µM concentration), 1µL of Qiagen Taq PCR buffer, 2µL of Q Solution and 0.1µL of Taq polymerase. Amplification reactions were conducted according to manufacturer's instructions. Reactions were run in an Eppendorf Mastercycler ep gradient S thermal cycler. 2µL of sample was run in a 1% agarose gel electrophoresis and in 1% TAE Buffer.

Table 3: Primers

Name	Oligonucleotide Sequence	Purpose
SC003	GGCGTAGAGGATCTGCTCATGTTTG	External to MCS in pDA12, forward
SC004	GCTACTGCCGCCAGGCAAATTCTGT	External to MCS in pDA12, reverse
SC137	CCAGTTCTAGACGTTCGAGCAGTTTCATCCA	*paaK1* upstream forward
SC140	CATTTGATATCGAGGCGTTCTTCCTGCA	*paaK1* downstream reverse
SC141	AACTCTCTAGAATCCAGCAGGAACTCGTCAA	*paaK2* upstream forward
SC142	CTTTGTCTAGAATGGCGTGATGTCGTTATC	*paaK2* upstream forward
SC143	CAGAATGGTACCGCCGTTCTACCCGAGGAAAC	*paaK2* downstream reverse
SC144	GCAGTGATATCTTCGAGCGTGTCGTCGAGCG	*paaK2* downstream reverse
SC153	GTGGATGACCTTTTGAATGACCTTT	External to MCS in pGPI-*Sce*I, forward
SC154	ACAGGAACACTTAACGGCTGACATG	External to MCS in pGPI-*Sce*I, reverse
SC164	CGCAGGTCGTTCTTGGTCGAGAA	*paaK2* upstream reverse
SC165	GCCAGTTCCAGATCACGCTGTCG	*paaK2* downstream reverse
SC166	GCGTGCAACTCGTACAACCTGAGTG	*paaK1* upstream forward
SC167	CGGATGTGGCTGCTGTTCCCGAATT	*paaK1* downstream reverse
SC168	ATGGAGAAGGGCGTGAACTATCCGT	*paaK2* upstream forward
SC169	ATCGCTGGCTATCACGATGTCGCAG	*paaK2* downstream reverse
SC172	GAGACACATATGACTACCCCGCTACCGCT	*paaK1* 5’
SC173	AACGTCTAGATCAGCCCTTGCGCTTGTCGA	*paaK1* 3’
SC176	CACGGTGAACCAGGGCGTGTG	pRL7 sequencing primer forward
SC177	CGACCGTCCGAACGCAGC	pRL7 sequencing primer reverse
SC210	ACAGTGATATCCCCGAGACGCAAAATACGGC	*paaK2* downstream reverse
SC211	TGGAGGAGCACCCCGATGTCGAGGTGTGCCGTT	*paaK2* downstream forward with homology region
SC212	AACGGCACACCTCGACATCGGGGTGCTCCTCCA	*paaK2* upstream reverse with homology region
SC232	ACCCATTTATGGGAGCACAG	BCAS OriC forward
SC233	TGCTCCAGCATCACTTTCAC	BCAS OriC reverse
SC234	ATGGGGTTCGTCTTTCTGTG	BCAS OriC forward
SC235	AGACCGATCTTTCCGGACTT	BCAS OriC reverse
SC242	CGACTATGCGGAAGGCGTGC	*paaI* upstream forward
SC243	CTCCAGTGTTTGTTATGGGC	*paaI* downstream reverse

Restriction sites are underlined

3.9. Creation of PaaK Deletion Mutants.

RJL1 (*paaK1* deletion mutant) was created by Robyn Law using the techniques outlined in Flannagan et al. using *B. cenocepacia* wild type K56-2 from the Valvano stock STC157 (Table 2) (Figure 7) (Law, 2009). For the purpose of this project, the same process was repeated on another K56-2 clone from the Valvano stock (STC300). The resulting mutant was called IAI1. This was done by tri-parental mating first with pRL5 which contains the upstream and downstream regions (bps) of paaK1 as well as a yeast I-*Sce*I restriction site (TAGGGATAACAGGGTAAT). Homologous recombination (and orientation of recombination) of the respective upstream and downstream regions were confirmed by colony PCR with primer pairs which anneal to the plasmid and the genome (SC154/SC165 and SC153/SC164). Following homologous recombination of the plasmid upstream/downstream with the genomic upstream/downstream, a second plasmid pDAI-*Sce*I which constitutively expresses the yeast homing endonuclease I-*Sce*I was introduced. Cleavage at the yeast restriction site favours intra-genomic recombination of the plasmid copy and the native genomic copies of the *paaK 1* upstream and downstream regions which results in the exclusion of *paaK1 I* and the DHFR marker from pRL5. Resulting clones were screened for trimethoprim sensitivity and tetracycline resistance by replica plating on LB with 100µg/ml tetracyline with and without 100µg/ml trimethoprim. Subsequently, TCs clones were screened for the deletion of *paaK1* (SC166/SC167). Following confirmation by colony PCR that the gene had been deleted, pDAI-*Sce*I was cured by serial dilution in LB broth as outlined by (Flannagan et al., 2008) with an additional dilution step. Loss of the plasmid was confirmed by colony PCR using SC003 and SC004 which anneal external to the multi-cloning site.

Creation of a *paak2* deletion mutant was attempted by construction of a new *paaK2* deletion plasmid via fusion overlap PCR. Briefly, the upstream and downstream regions were cloned independently with two sets of primers of which upstream reverse primer and the downstream forward primer were designed to have sequence homology. A second amplification using equal amounts of purified upstream and downstream product, using the outside primers, should have resulted in a single fusion product which would then have been ligated into the backbone plasmid pGPI-*Sce*I to make the deletion plasmid. The resulting plasmid is then introduced by triparental mating into the wild type strain K56-2 in the same manner as the *paaK1* equivalent pRL5.

Fig. 7. **Targeted Non-polar Mutagenesis Deletion Scheme** for the clean deletion of genes in *Burkholderia cenocepacia.* Consisting of (Step1) Constructing the deletion plasmid by cloning the target gene upstream and downstream regions onto the pGPI-*Sce*I backbone and introduction of the deletion plasmid by triparental mating and homologous recombination; (Step2) Cleavage at I-*Sce*I site by pDAI-*Sce*I constitutively expressed yeast endonuclease; Step 3 Second homologous Recombination and exclusion of target gene. (Flannagan et al., 2008)

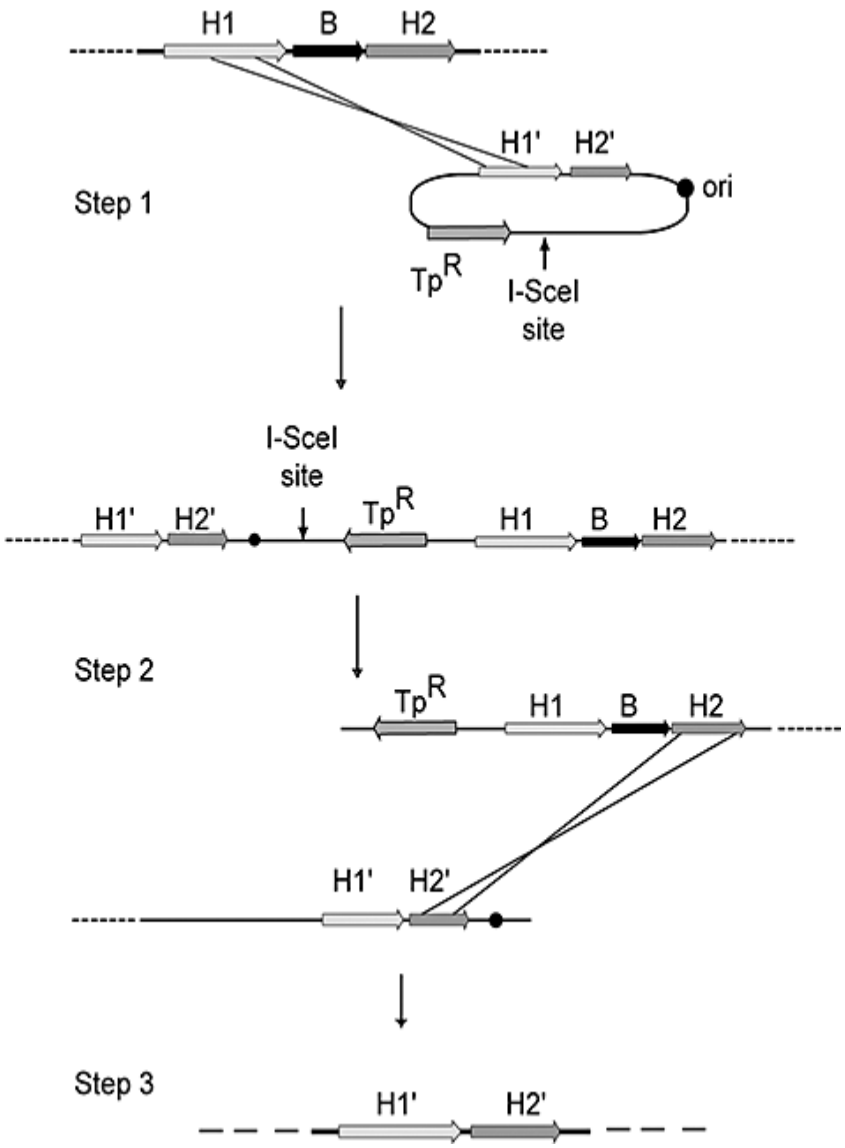
H1
B
H2
H1'
H2'
ori
Step 1
TpR
I-SceI
site
I-SceI
site
H1'
H2'
TpR
H1
B
H2
Step 2
TpR
H1
B
H2
H1'
H2'
Step 3
H1'
H2'

3.10. Reporter Activity Assays

Reporter assays were done in 96-well format M9 media supplemented with 0.1% glycerol (to ensure growth and to prevent catabolite repression in favour of glucose) as well as 5mM of PA, 3-OHPA or 4-OHPA. The positive control media was M9 media plus 25mM glycerol. Reporter plasmids pJH1, pJH2, and pJH7 were introduced by triparental mating (see Section 3.5). 1.5ml of overnight culture was washed once in PBS solution and then resuspended in 1.5ml of the same. The number of cells in a 20µL at an OD600nm of 2 was inoculated into a 1mL eppendorf tube of media and mixed well. Of the latter, 150µL aliquots were added to wells in triplicate. The cells were grown at 37^{o}C for 24 hrs in a Biotek 2 Plate reader with OD 600nm and fluorescence readings taken hourly. Relative fluorescence was calculated as a measure of raw fluorescence over growth (OD600nm) and plotted against time (hrs).

3.11. Complementation Analysis of RJL1

RJL1 was complemented with *paaK1* by tri-parental mating with donor *E. coli* DH5α pDA12*paaK1* and helper strain *E. coli* pRK2013. Resulting colonies were screened by colony PCR with primers SC003 and SC004 and primers SC172 and SC173. The resulting strain was compared with RJL1 in a slow killing assay.

3.12. Comparative Sequencing of RJL1 and IAI1

RJL1 and IAI1 were grown overnight on LB agar. Primers 242 and 167, which flank the *paaI* and *paaK1* regions in K56-2, were used to amplify an 880 bp fragments which was gel purified (Qiagen gel purification kit) and then sent to the TCAG centre to be sequenced using primers

SC242, SC243, SC166 and SC167. The sequences were aligned using the Align-X tool featured in Vector NTI and the Finch-TV chromatogram provided by the TCAG center at the Sick Kids Foundation. Reverse sequences were reverse complemented before comparisons. Comparisons for each mutant were made to the *B. cenocepacia* J2315 genome and to the other mutant (Holden et al., 2009).

4. Results

4.1. PaaK1 and PaaK2 are both independently functional and complement the E. coli PaaK

The PA pathway is well conserved among bacterial microorganisms. *B. cenocepacia* has two *paaK* genes. In order to analyze the level of cross-specific conservation of *E. coli paaK* relative to our subject strain, *B. cenocepacia paaK1* and *paaK2* were each cloned onto the backbone of pDA12 (Courtesy of Dr. Boulanger) and introduced into a *paaK* defective *E. coli* W strain (W14pAADTn1000-46; see Table 2) (Ferrandez et al., 1998). Because PaaK2 is challenging to clone (due to a high GC content inter alia), the *paaK2* insert was synthesized and codon optimized by converting every third base from a glycine or cytosine to an adenine or thymine to account for the high GC content in *B. cenocepacia* relative to *E. coli*. The resulting strain was grown in 5mL test tubes containing M63 minimal media with PA and glycerol over 24 hours. Figure 8 shows a comparison of growth in PA and in glycerol. The wild type like strain grows in both carbon sources. The vector control and the PaaK$^-$ strain show reduced growth in PA whereas the growth of the complemented strains shows growth in PA. Growth of the strains harboring the *B. cenocepacia paaK1* or *paaK2* was calculated as a percent of the wild type like strain (W14pAAD) growth (Figure 9). Both complemented strains grew in PA. The *paaK1* gene complemented the paak defective *E. coli* strain to 62.2% of wild type growth in PA while the *paaK2* complement restored 98.5%. The negative control (W14pAADTn1000-46) and the vector control restored growth in PA to only 14% and 12.5% respectively.

Fig. 8. ***B. cenocepacia paaK1* and *paaK2* are each independently functional.** *B. cenocepacia paaK1* and *paaK2* was introduced *in trans* (on pDA12 backbone) in *paaK* defective strain *E. coli* W 14pAADTn1000-46. Strains were grown in M63 minimal media supplemented with 5mM PA and 0.1% glycerol at 30^{o}C for 24 hours

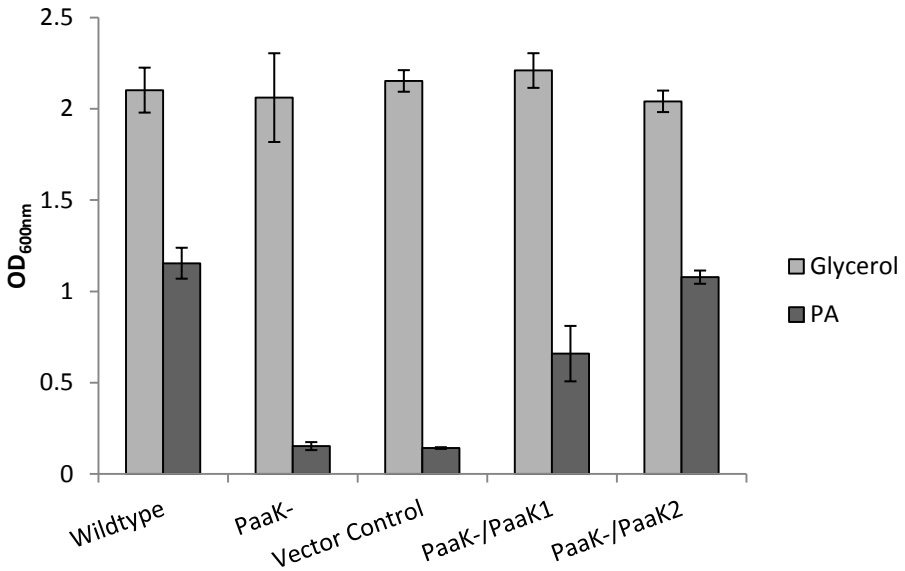
2.5
2
1.5
1
0.5
0
OD600nm
Glycerol
PA
Wildtype
PaaK-
Vector Control
PaaK-/PaaK1
PaaK-/PaaK2

Fig. 9. ***B. cenocepacia paaK2 complements better in E. coli W than B. cenocepacia paaK1.*** *B. cenocepacia paaK1* and *paaK2* was introduced *in trans* (on pDA12 backbone) in *paaK* defective strain *E. coli* W 14pAADTn1000-46. Strains were grown in M63 minimal media supplemented with 5mM PA and 0.1% glycerol at 30^{o}C for 24 hours. Percent growth comparison of *paaK1* complement and *paaK2* complement with *E. coli* wild type like strain.

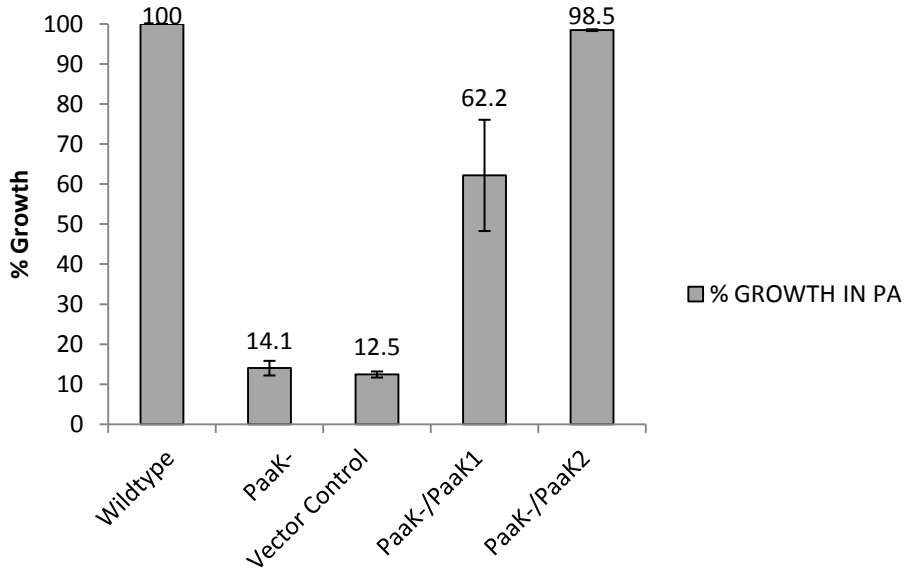
100
98.5
62.2
14.1
12.5
% Growth
100
90
80
70
60
50
40
30
20
10
0
Wildtype
PaaK-
Vector Control
PaaK-/PaaK1
PaaK-/PaaK2
% GROWTH IN PA

4.2. Creation of PaaK Deletion mutants and Double Deletion mutant

The original intent of this project was to construct the double deletion mutant by deleting *paaK1* on the background of a pre-made *paak2* deletion mutant FJK2. However, it became necessary to make another *paaK2* deletion mutant when colony PCR of FJK2 (with primers SC141 and SC144; Table 3) revealed a wild type band demonstrating that it was a wild type revertant. This was done using triparental mating on the wild type background with pRL7 the *paaK2* deletion plasmid (Law, 2009). More colonies were observed having downstream than upstream recombination and even these colonies did not have a deletion band (primer pairs SC153/SC164 and SC154/SC165 for upstream and downstream respectively) after the second tri-parental mating with the mutagenesis plasmid pDAI-*Sce*I. Sequencing of pRL7 revealed a ~400bp section was missing from the beginning portion of the *paaK2* upstream flanking region which accounted for the seeming predisposition toward downstream recombined colonies and suggests that the reason primer pair SC153/SC164 did not result in any bands is because SC164 annealing region was absent. Additionally, pRL7 was missing a single base (A), which overlaps as a stop codon in the downstream flanking region and the first base in the start codon of downstream gene *paaH*. Consequently, using this plasmid, even without the missing section, would have resulted in a polar mutation.

Due to these developments, it became necessary to make a new *paaK2* deletion plasmid. Rather than clone the upstream individually and sequentially as was done previously (Law, 2009) we adopted the fusion PCR overlap approach proposed by Dubarry et al (2010) and explained in the Materials and Methods section 3.10(Dubarry et al., 2010). Despite acquiring clean high yield upstream and downstream products using Hotstar Hi-Fidelity Polymerase, we ran into difficulties cloning fusion/overlap PCR resulting in a lot of unspecific banding and a low

product yield. The actual PCR reaction was highly inconsistent despite many attempts at optimizing the reaction for the temperature. Following amplification of fusion product, it was to be ligated into pGPI-*Sce*I backone between the XbaI and EcoRV restriction sites. The ligation failed due to the low DNA concentration of the insert and due to the fact that the fusion PCR could not be optimized, a decision was made to focus on the *paaK1* deletion mutant.

4.3. Growth of IAI1(paaK1 deletion mutant) in PA

The second *paaK1* deletion mutant IAI1was grown in minimal media supplemented with PA or glucose. As seen in Figure 10, the wild type strain K56-2 grew in both PA and glucose whereas insertional mutants *paaA* (STC 179) and *paaE* (STC155) did not grow in PA. IAI1 (shown as *paaK1*) grows in the presence of PA improved upon wild type growth by 31% percent growth. This is likely accounted for by the presence of a functional *paaK2* gene.

4.3.1. B. cenocepacia grows in ring-substituted PA derivatives 3-OHPA and 4-OHPA

Our overall hypothesis is that the two ligases may be differentiated by a preference for aromatic substrates. Crystallographic studies demonstrated that PaaK1 and PaaK2 can be differentiated based on the size of the substrate binding pocket (Law and Boulanger, 2011). Specifically, the PaaK1 binding pocket is larger because of an alanine residue at the base compared to a bulky isoleucine in the PaaK2 binding pocket (Figure 11). In order to investigate the use of 3-OHPA and 4-OHPA as substrates for *B. cenocepacia*, we grew the wild type strain K56-2 using each of the compounds as sole carbon sources in M9 minimal media including PA and glucose as controls. PA pathway mutants for monooxygenase complex subunits PaaA and PaaE and PaaK1 (IAI1) were also included to relate metabolism of 3-OHPA and 4-OHPA to the

PA pathway (Figure 12). For K56-2, we observed growth in all carbon sources in comparison to glucose (positive growth control) with up to 85% growth in PA, 80% in 3-OHPA and 65% in 4-OHPA . Conversely in *paaA* and *paaE* mutants we had less than 4% growth in PA but up to 60% and 50% in 3-OHPA and 4-OHPA respectively. IAI1 had higher than wild type growth at 110% growth in PA as well as in 3-OHPA and 4-OHPA with 88% and 80% respectively.

Fig 10. **Growth of *B. cenocepacia paaK1 deletion mutant* with PA as a sole carbon source.** *B. cenocepacia* K56-2 (wild type), deletion mutant IAI1 (*paaK1*), and insertional mutants STC179, (*paaA*) and STC155 (*paaE*) were grown for 24 hr in M9 media supplemented with 5mM PA or 0.2% glucose as sole carbon sources.

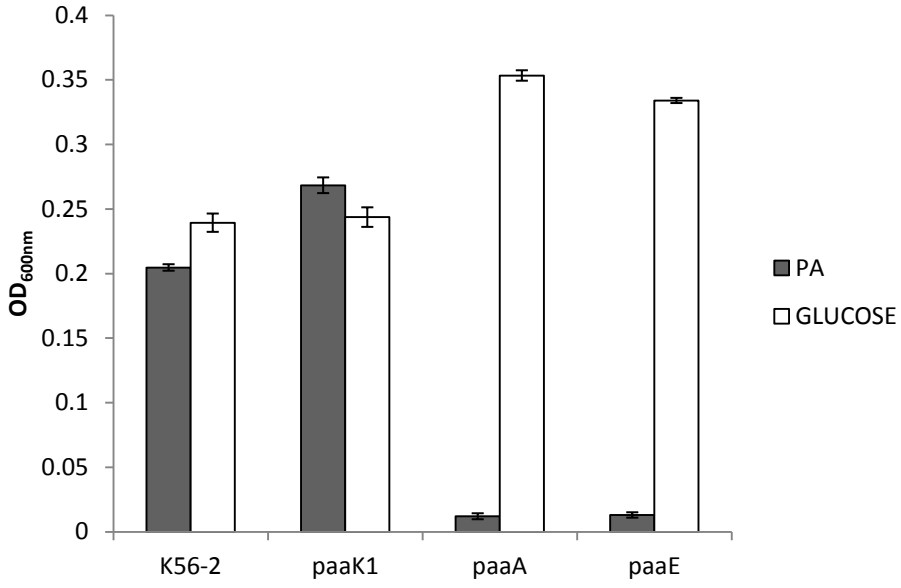
0.4
0.35
0.3
0.25
0.2
0.15
0.1
0.05
0
OD600nm
K56-2
paaK1
paaA
paaE
PA
GLUCOSE

Fig. 11. ***B. cenocepacia paaK1*** **and** ***paaK2*** **Crystal Structures of the Substrate Binding Pockets.** Graphic representations of the crystal structures of the substrate binding pockets of PaaK1 and PaaK2 showing the Ala-Ile difference in PaaK1 and PaaK2 respectively. (Law and Boulanger, 2011)

PaaK1

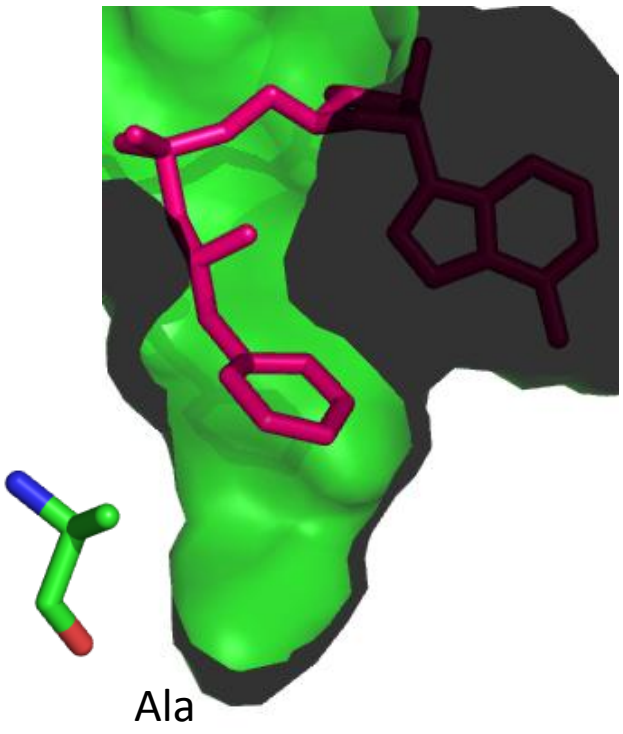

Ala

PaaK2

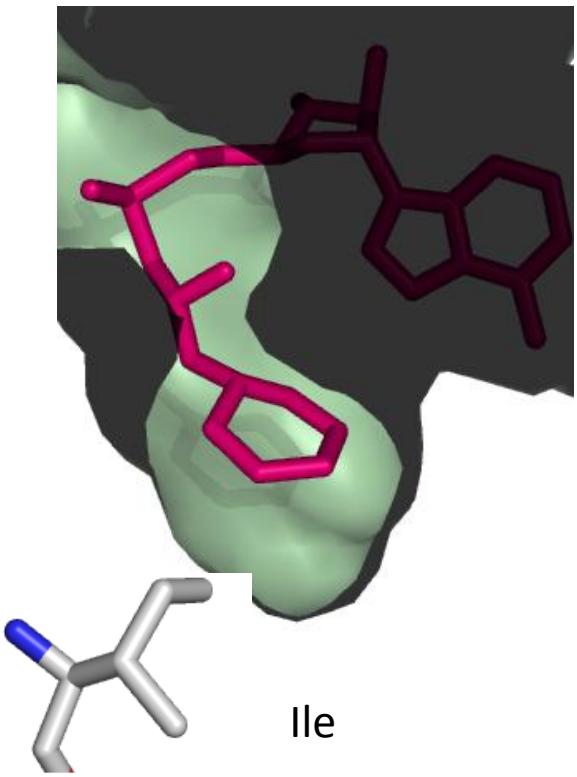

Ile

Fig 12. **Growth of *B. cenocepacia* strains with 3-OHPA, 4-OHPA as sole carbon sources.** *B. cenocepacia* K56-2 (wild type), deletion mutant IAI1 (*paaK1*), and insertional mutants STC179 (*paaA*) and STC155 (*paaE*) were grown for 24 hr in M9 media supplemented with 5mM PA, 3-OHPA, 4-OHPA or 0.2% glucose as sole carbon sources.

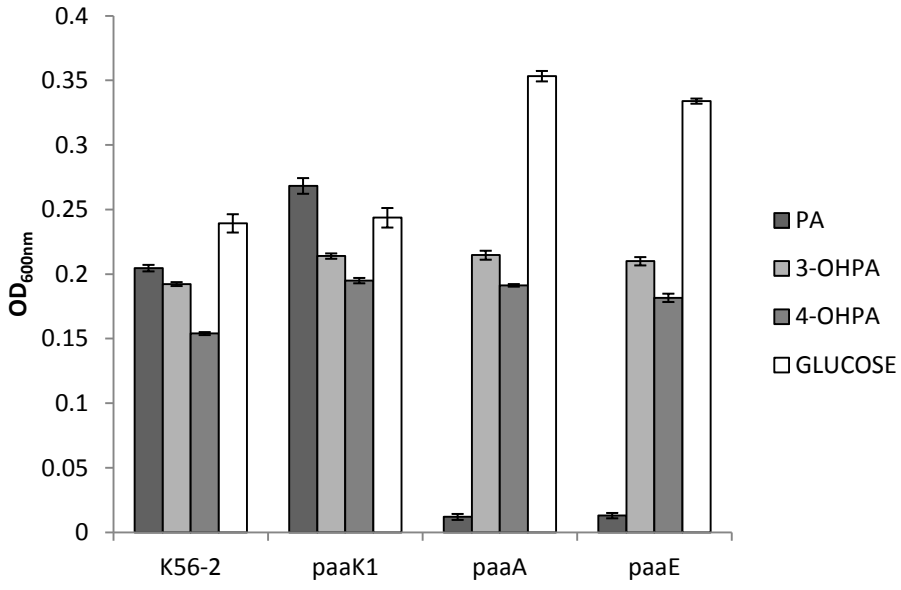
0.4
0.35
0.3
0.25
0.2
0.15
0.1
0.05
0
OD600nm
K56-2
paaK1
paaA
paaE
PA
3-OHPA
4-OHPA
GLUCOSE

4.4. 3-OHPA Induces the PA degradative pathway

Previous enzyme kinetics assays reported by Law et al. 2011, demonstrated that PaaK1 is able to bind 3-OHPA better than PaaK2 and can exclusively bind 4-OHPA compared to PaaK2. We reasoned that 3-OHPA and 4-OHPA, as substrates for PaaK1, could induce the PA degradative pathway in *Burkholderia cenocepacia*. In order to test this concept, we utilized a PA pathway induction reporter assay previously developed in our laboratory (Hamlin et al., 2009). The translational reporter consists of a plasmid with the enhanced green fluorescent protein gene (e-*gfp*) controlled by the *paa* promoter for each of the three *paa* gene clusters of the *B. cenocepacia paa* operons that start with the *paaZ*, *paaA* and *paaH* genes. Growth of a strain carrying the reporter plasmid in minimal media with PA results in expression of eGFP, which can be measured by fluorescence as an indication of the induction of the PA pathway. Plasmids pJH1 and pJH2 carry *e-gfp* under control of the constitutive expression promoter *DHFR* and a promoterless *e-gfp*, respectively.

B. cenocepacia K56-2 reporter strains were grown in M9 minimal media with glycerol supplemented with 5mM PA, 3-OHPA, or 4-OHPA. After 24 h of incubation at 37°C the relative fluorescence of wild type and reporter strains was analyzed. The results are shown in Figure 13. Low levels of background fluorescence were observed for *B. cenocepacia* K56-2 wild type and the reporter strain carrying a promoter-less *e-gfp* gene. On the contrary, when *B. cenocepacia*/pJH1 was grown with glycerol or glycerol plus phenolic acids, increased fluorescence was observed. The levels of relative fluorescence due to PA, 3-OHPA, or 4-OHPA were comparable suggesting that there are no metabolic effects of these compounds on plasmid copy number. When PA pathway reporter strains were grown in the presence of PA, an increase in relative fluorescence was observed as previously described. However, only 3-OHPA but not

4-OHPA was capable of inducing the *paaZ*, *paaA* and *paaH* promoters while the relative fluorescence due to 4-OHPA was comparable to the one in the presence of only glycerol (Fig.11). Across the board, we noted an average of 5 times less relative fluorescence in media containing 4-OHPA than in media containing PA and relative fluorescence levels were similar to negative controls. Interestingly, *B. cenocepacia* K56-2/pJH6 registered a two-fold increase in relative fluorescence for 3-OHPA than PA (7389 and 4281 respectively). However this was not the case for *B. cenocepacia* K56-2 harboring pJH7 or pJH8. None of the other reporter strains showed a significant difference in relative fluorescence in response to PA compared to 3-OHPA (11206 and 9966 units, respectively for pJH7 and 4454 and 3502 units, respectively for pJH8). For all carbon sources tested, pJH7 registered a phenotype characterized with strongest levels of relative fluorescence compared to the other reporter strains. This has been suggested to be an indicator of the importance of PaaA or the monooxygenase complex in the PA degradative pathway (Hamlin et al., 2009).

Fig. 13. ***B. cenocepacia* K56-2 Reporter Activity Assays.** PA pathway induction in *B. cenocepacia* K56-2 (wild type) measured as relative fluorescence at 12 hr. Strains were grown in M9 minimal media with PA, 3-OHPA, or 4-OHPA (plus 0.1% glycerol) or 0.2% glycerol. pJH7, *paaA* promoter reporter; pJH8, *paaH* promoter reporter; pJH6, *paaZ* promoter reporter; pJH1, positive control; pJH2, negative control.

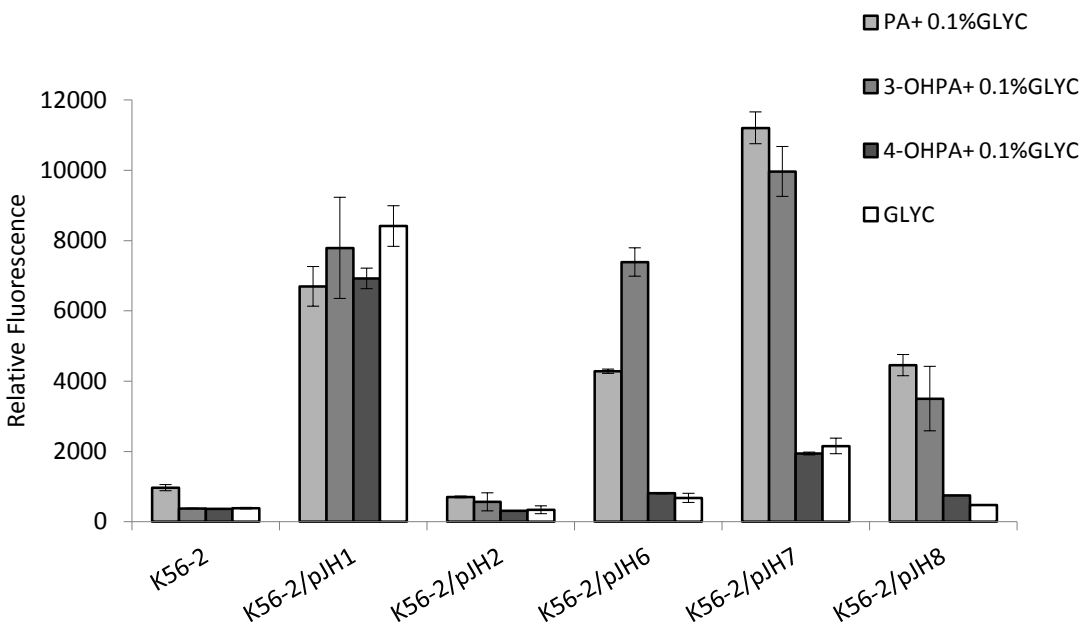
PA+ 0.1%GLYC
3-OHPA+ 0.1%GLYC
4-OHPA+ 0.1%GLYC
GLYC
Relative Fluorescence
12000
10000
8000
6000
4000
2000
0
K56-2
K56-2/pJH1
K56-2/pJH2
K56-2/pJH6
K56-2/pJH7
K56-2/pJH8

4.4.1. 3-OHPA induction of the PA degradative pathway is PaaK1 dependent

In order to shed light on the role of *paaK1* gene in the induction of PA degradation by 3-OHPA, we constructed a *B. cenocepacia* K56-2 *paaK1* deletion mutant, IAI1 and introduced the reporter plasmid pJH7 in this strain. Next, the relative fluorescence of the reporter system due to induction by 3-OHPA in the *paaK1* genetic background was compared that of the wild type. Figure 14 shows an increase in relative fluorescence in the presence of PA in both wild type and IAI1 reporter strains. This is expected due to the presence of at least one functioning *paaK* gene (Law et al., 2008). It is probable then, that the PaaK2 enzyme is able to synthesize the PA-CoA, which is necessary to activate the *paa* promoters (Yudistira et al., 2011). Nevertheless, compared to K56-2/pJH7, IAI/pJH7 has 10% less fluorescence possibly due to the presence of two functioning ligases in the wild type variant compared to one in the mutant (Figure 15). K56-2/pJH7 registered induction of the PA degradative pathway in 3-OHPA, (but not 4-OHPA) converse to IAI1/pJH7, which did not for either carbon source. We can therefore deduce that induction of the PA degradative pathway by 3-OHPA is dependent on the presence of PaaK1 and not PaaK2.

Fig. 14. ***paaK1 deletion mutant(IAI1) Reporter Activity Assays.*** *paaA* promoter induction in *B. cenocepacia* K56-2 (wild type) and *B. cenocepacia* deletion mutant IAI1 (*paaK1*) measured as relative fluorescence at 12 hr. Strains were grown in M9 minimal media with PA, 3-OHPA, or 4-OHPA (plus 0.1% glycerol) or 0.2% glycerol. pJH7 is the *paaA* promoter reporter plasmid. Note that the large error bars for IAI1/pJH7 and K56-2/pJH7 in M9 minimal media plus 0.2% glycerol are due to outliers in one replicate.

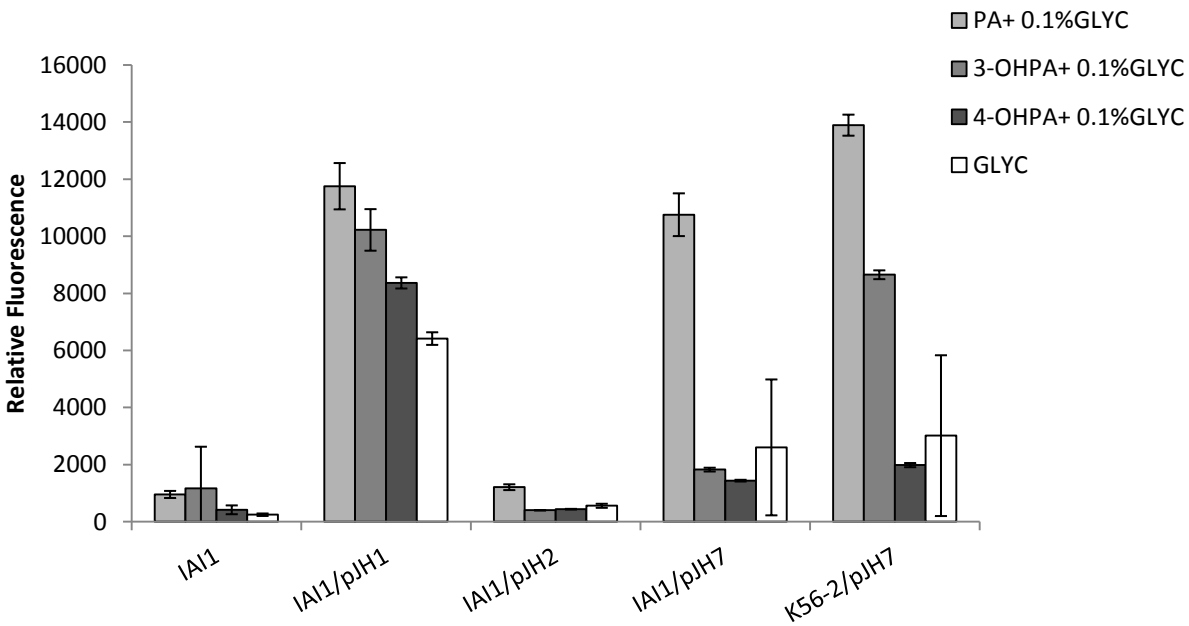
PA+ 0.1%GLYC
3-OHPA+ 0.1%GLYC
4-OHPA+ 0.1%GLYC
GLYC
Relative Fluorescence
16000
14000
12000
10000
8000
6000
4000
2000
0
IAI1
IAI1/pJH1
IAI1/pJH2
IAI1/pJH7
K56-2/pJH7

Fig. 15. ***paaK1* Reporter Activity Assays-Comparison of K56-pJH7 and IAI1pJH7.** *paaA* promoter induction in *B. cenocepacia* K56-2 (wild type) and *B. cenocepacia* deletion mutant IAI1 (*paaK1*) measured as relative fluorescence at 12 hr. Strains were grown in M9 minimal media with PA, 3-OHPA, or 4-OHPA (plus 0.1% glycerol) or 0.2% glycerol. pJH7, *paaA* promoter reporter plasmid. Note that the large error bars in the M9 minimal media plus 0,2% glycerol for both strains are due to outliers in one replicate for each strain.

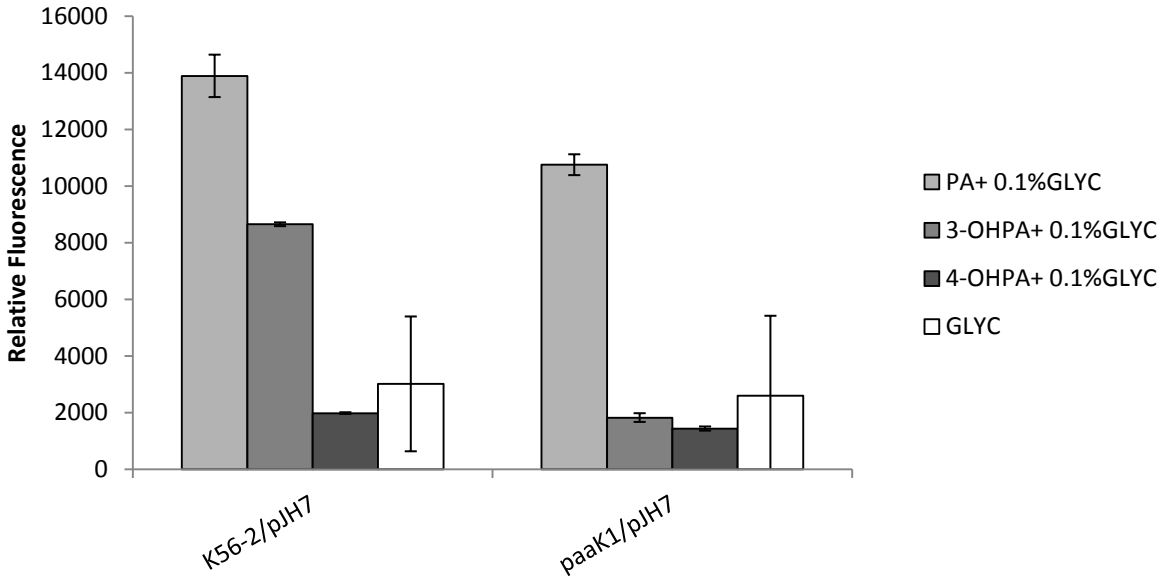
16000
14000
12000
10000
8000
6000
4000
2000
0
Relative Fluorescence
K56-2/pJH7
paaK1/pJH7
PA+ 0.1%GLYC
3-OHPA+ 0.1%GLYC
4-OHPA+ 0.1%GLYC
GLYC

4.5. Complementation of paaK1 in RJL1 does not restore pathogenicity.

Previously, RJL1 a paaK1 deletion mutant was made using targeted nonpolar mutagenesis (Flannagan et al., 2008) on the background of STC 157 a K56-2 wild type clone. *In vivo* analysis of this strain by slow killing assays revealed attenuated killing of nematode *C. elegans* seemingly linking PaaK1 to pathogenicity. We aimed to support this assertion by complementing *paaK1* into RJL1 *in trans* using pDA12*paaK1* (Table 2) by tri-parental mating. The identity of the new strain was confirmed by colony PCR using primer pairs SC003 and SC004 and SC172 and SC173 which anneal to the multi-cloning site of the plasmid and the outer regions of the *paaK1* sequence respectively.

4.5.1. In vivo analysis of paaK1 complemented strain

Following construction of the complemented strain (RJL1/ pDA12paaK1), a nematode killing assay was conducted to assess pathogenicity. RJL1 has an attenuated phenotype compared to the wild type strain (Figure 16B) (Law, 2009). However, there was no significant difference between the background strain RJL1 and the complemented strain RJL1/pDA12*paaK1* (p value=0.0951 where > 0.05 is statistically significant; Figure 16A). Similarly, there was no significant difference between the complemented strain and the empty vector control RJL1/pDA12 (p value=0.0588) confirming that the vector itself was not affecting the phenotype (See Figure17A). As expected, RJL1pDA12 shows a similar attenuated phenotype as RJL1 compared to the wild type strain (17B). Accordingly, we reasoned that since the attenuated pathogenicity phenotype in RJL1 could not be due to the loss of PaaK1 but due to a secondary mutation or a mutation to the particular parent wild type strain (STC 157).

Fig. 16. **Complementing paaK1 in RJL1 does not restore pathogenicity** Kaplan Meier Survival curve comparing killing phenotypes of (A) *paaK1* deletion mutant, RJL1 (n=114; broken line) and *paaK1* complemented RJL1 (n=112; solid line) . (P value =0.0951, NS.) (B) wild type strain K56-2 (n=103; solid line) and *paaK1* deletion mutant, RJL1 (n=114; broken line). (P value =0.0001)

A

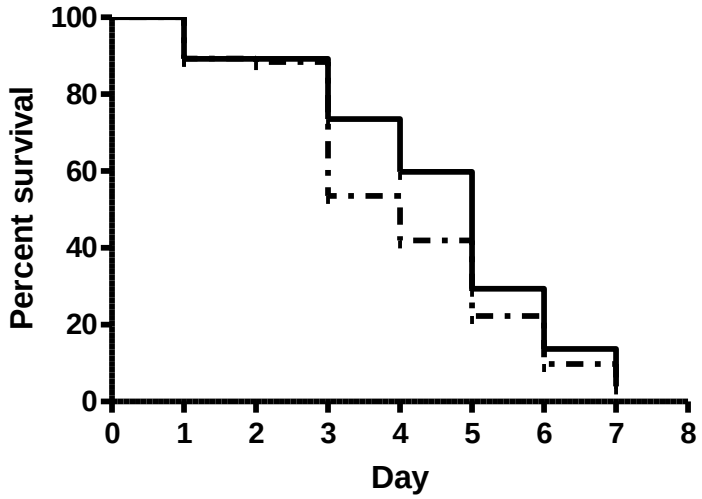
Percent survival
100
80
60
40
20
0
0 1 2 3 4 5 6 7 8
Day

B

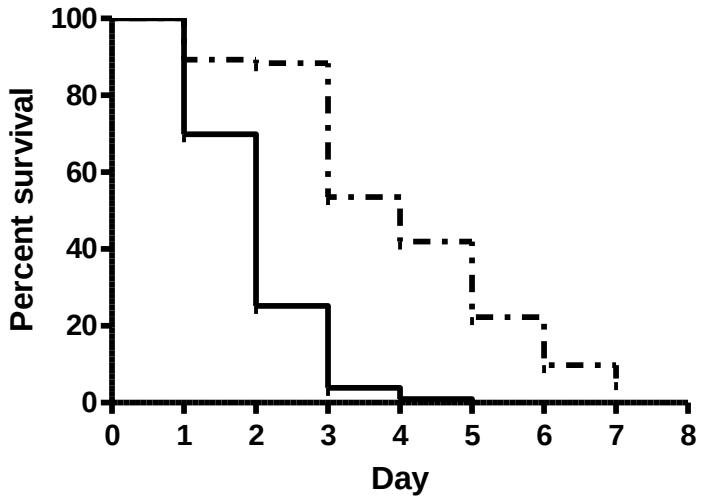
Percent survival
100
80
60
40
20
0
0 1 2 3 4 5 6 7 8
Day

Fig. 17. **Complementing *paaK1* in RJL1 does not restore pathogenicity (Vector Control).** The vector pDA12 has no significant effect on strain pathogenicity. Kaplan Meier Survival curve comparing killing phenotypes of (A) *paaK1* deletion mutant RJL1 (n=114; solid line) and *paaK1* deletion mutant vector control, RJL1/pDA12 (n=113; broken line). P value = 0.0588, NS. (B) Wild type strain K56-2 (n=103; solid line) and *paaK1* deletion mutant/vector control, RJL1/pDA12 (n=113; broken line). P value =0.0001, S.

A

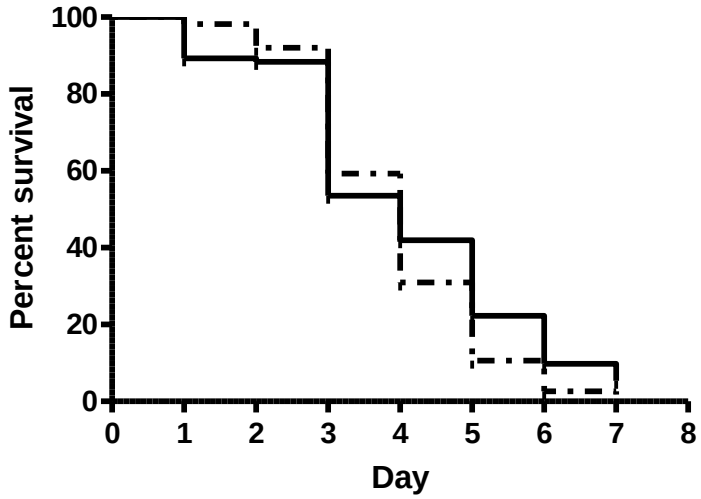
Percent survival
100
80
60
40
20
0
0 1 2 3 4 5 6 7 8
Day

B

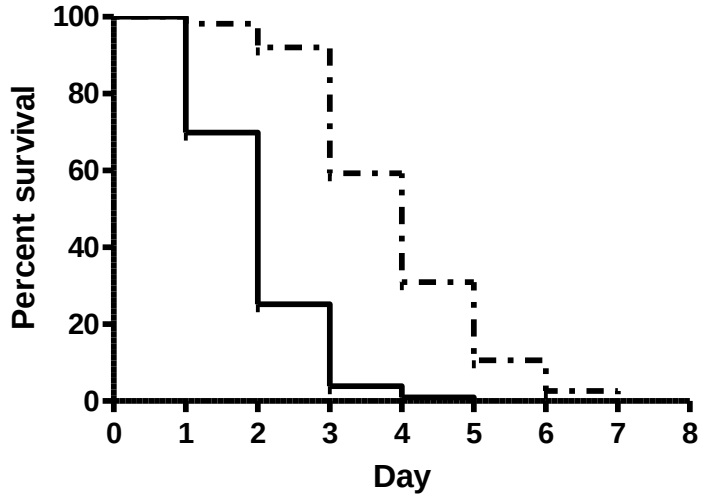
Percent survival
100
80
60
40
20
0
0 1 2 3 4 5 6 7 8
Day

4.5.2. Deletion of PaaK1 does not result in attenuated pathogenicity

In order to account for a possible secondary mutation in RJL1, we made another *paaK1* deletion mutant on STC300, the K56-2 wild type isolate from which STC157 was sub-cloned. Once again, deletion plasmid pRL5 (used to make RJL1) was introduced via tri-parental mating (Figure 7, 18). The resulting strain and the orientation of recombination were confirmed using primer pairs SC153/SC164 (upstream flanking recombination) and SC154/SC165 (downstream flanking recombination). Introduction of pDAI*Sce*I resulted in paaK1 deletion clones (Figure 19) which were cured of the plasmid by serial dilution (Flannagan et al., 2008). The resulting mutant (IAI1) was tested in vivo in a slow killing assay. The survival curve, shown in Figure 20A, revealed IAI1 to have wild type like pathogenicity registering no significant difference compared to the wild type (p value = 0.0063). Figure 20B illustrates a survival curve comparing IAI1 and RJL1 showing a significant difference (pvalue= 0.0001) between the two mutants that is similar to that of the RJL1/K56-2 comparison (Figure 21A; pvalue= 0.0001). A confirmatory comparison of two isolated IAI1 clones showed no significant difference in killing phenotype (Figure 21B p value=0.06646;).

Fig. 18. ***paaK1*** **Deletion plasmid pRL5.** Constructed by cloning the upstream (*paaK1*U) and downstream (*paaK1*D) flanking regions of *paaK1* .Constructed by Robyn Law (Law, 2009)

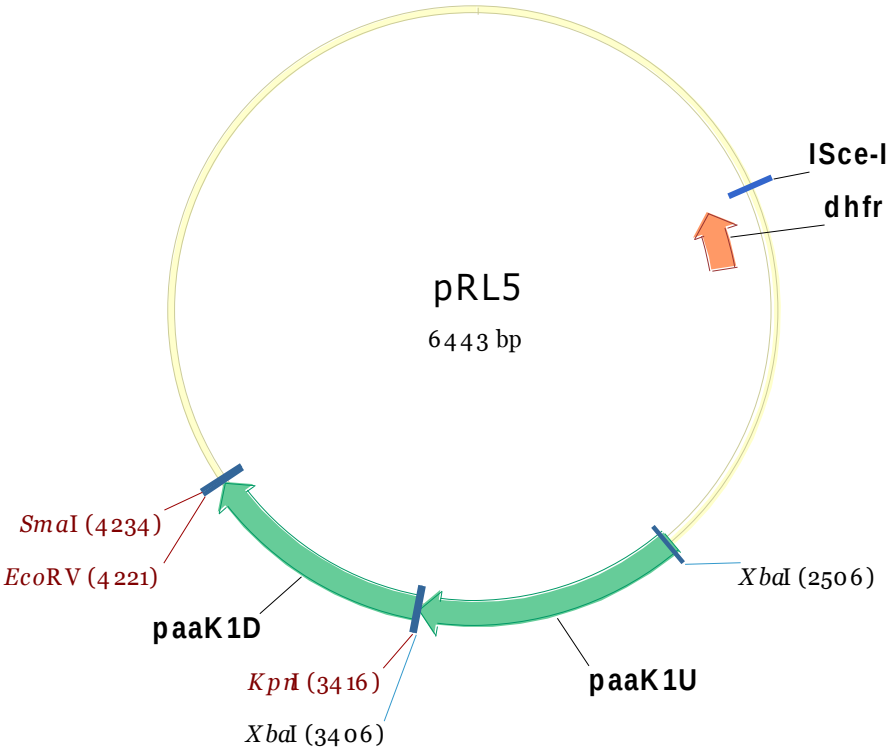
ISce-I
dhfr
pRL5
6443 bp
SmaI (4234)
EcoRV (4221)
paaK1D
KpnI (3416)
XbaI (3406)
paaK1U
XbaI (2506)

Fig. 19. **Construction of PaaK1 deletion mutant**

PCR confirmation of 10 *paaK1* deletion mutant clones #34-#90(551bps) compared to the wildtype strain and *paaK1* RJL1. #34 and #60 were selected at random for further experiments. Note the light wild type (WT) band at 1850bps compared to RJL1 which also has 551bps.

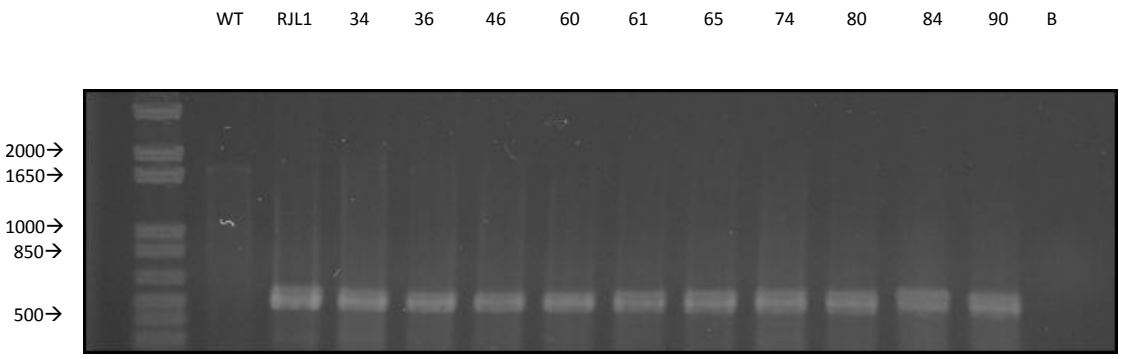
WT
RJL1
34
36
46
60
61
65
74
80
84
90
B
2000→
1650→
1000→
850→
500→

Fig. 20. **Paak1 deletion mutant IAI1 has a wildtype pathogenicity compared to RJL1.** Kaplan Meier Survival curve comparing killing phenotypes of (A) Two *paaK1* deletion mutants RJL1 (n=113; solid line) and, IAI1 (n=110; broken line) in a *C. elegans* Slow Killing assay. P value =0.0001, (B) wild type strain K56-2 (n=113; solid line) and *paaK1* deletion mutant, RJL1 (n=110; broken line) in a *C. elegans* Slow Killing assay. P value =0.0001.

A

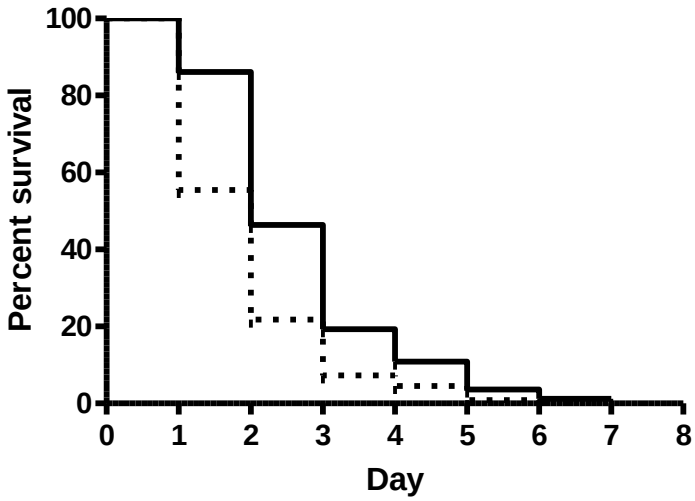
Percent survival
100
80
60
40
20
0
0 1 2 3 4 5 6 7 8
Day

B

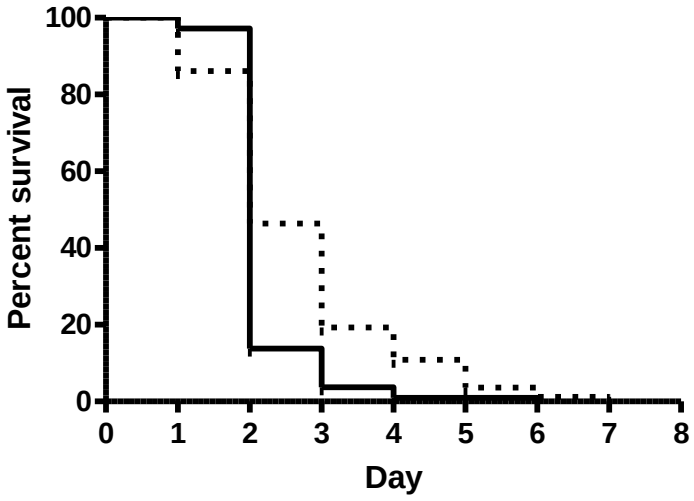
Percent survival
100
80
60
40
20
0
0 1 2 3 4 5 6 7 8
Day

Fig. 21. **Paak1 deletion mutant IAI1 has wild type pathogenicity compared to wild type.** Kaplan Meier Survival curve comparing killing phenotypes of A) Wild type strain K56-2 (n=113; solid line) and *paaK1* deletion mutant, IAI1 (n=110; broken line) in a *C. elegans* Slow Killing assay. P value =0.0063, NS. B) two *paaK1* deletion mutant IAI1 clones #34(n=110; broken line) and #60 (n=110; broken line) in a *C. elegans* Slow Killing assay. P value =0.06646 NS,.

A

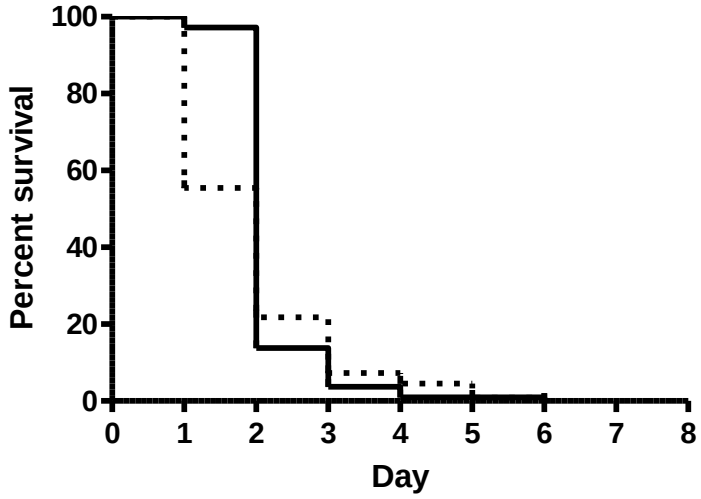
Percent survival
100
80
60
40
20
0
0 1 2 3 4 5 6 7 8
Day

B

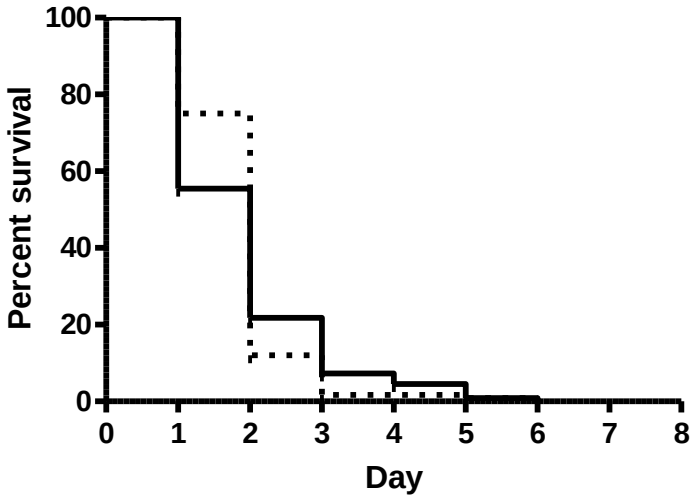
Percent survival
100
80
60
40
20
0
0 1 2 3 4 5 6 7 8
Day

4.6. Comparison of RJL1 and IAI1

It became necessary to compare RJL1 and IAI1 in order to investigate a possible secondary mutation causing the discrepancy in pathogenicity between the two otherwise phenotypically similar strains.

4.7. Possible loss of Chromosome 3

Based on a communications with the Eberl lab in Zurich, we entertained the possibility that the parent wild type strain for RJL1, wild type strain K56-2 -STC157 could have spontaneously lost Chromosome 3 or BCAS and that this loss could result in a loss of pathogenicity. In order to investigate this possibility, colony PCR was carried out on K56-2 -STC157, K56-2-STC300, and their respective *paaK1* deletion mutants, RJL1 and IAI1 utilizing two sets of primers (an external set SC232/SC23 -1075bp and an internal set SC234/235-750bps; sequences were provided by the Eberl Lab) flanking the chromosome 3 origin of replication. Figure 22 shows that Chromosome 3 registered expected bands for all four strains tested.

4.8. Possible Mutation in PaaI/Upstream flanking Region

Another option considered was a possible mutation in the *paaI* region. *paaI* is located just upstream of *paaK1*. It encodes the acyl-CoA thioesterase PaaI the only member of the *paa* operon which has no clearly defined function in the PA pathway. PaaI is a hotdog fold enzyme which releases the carboxylate part of an acyl-CoA molecule for further degradation and the CoA part for alternative metabolic pathways(Song et al., 2006). Because *paaI* is a small gene at only 452bps, it comprises a significant portion of the upstream flanking region cloned into pRL5.

The region between the beginning of the *paaI* region and the edge of the downstream section of the *paaK1* gene for IAI1 and RJL1 was amplified using primers SC242 (f), and SC167(r), purified and then sent to the TCAG centre for sequencing with the previous two primers and SC166 (f) SC243(r) (Table 2). Alignment of all sequences revealed as such as 96% sequence similarity with the J2315 genome (with paaK1 removed) (Figure 23). There was an inconsistent section located at the XbaI stitch between the upstream and downstream regions. However, this difference was identical for both *paaK1* mutants. A previous mutant, STC181, was made by insertional mutagenesis of paaK1 registered wild type levels of pathogenicity and growth in PA. For this reason, we can deduce that the attenuated phenotype in RJL1 is caused by a secondary mutation that has not yet been described.

Fig. 22. **Screening For Loss of Chromosome 3** in K56-2 wild type parent strains and their respective *paaK1* mutants**.** PCR confirmation of the presence of Chromosome 3 using two sets of primers (set 2 = *). 1) K56-2 (STC157) 2) K56-2 (STC300) 3) RJL1 pDAISceI 4) RJL1 5)IAI1 6) Blank (NOTE=Lane 2 set 1 is blank)

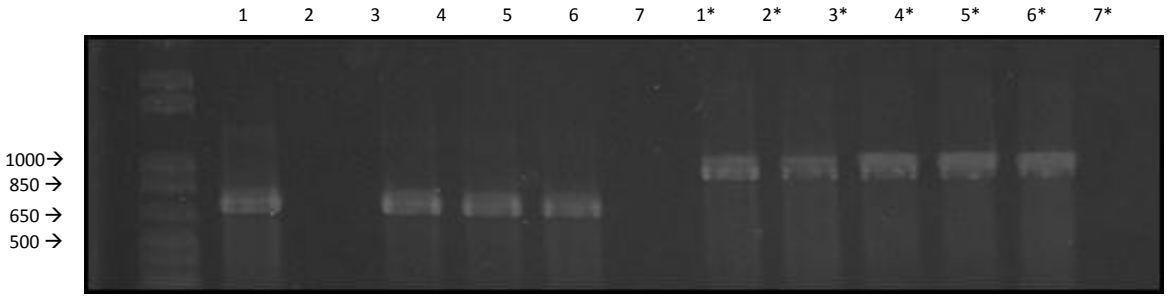
1
2
3
4
5
6
7
1*
2*
3*
4*
5*
6*
7*
1000→
850 →
650 →
500 →

Fig. 23. **Comparative Sequencing of RJL1 and IAI1.** Comparison of the paaI-paaK region of *B. cenocepacia* J2315 genome with that of *B. cenocepacia paaK1* deletion mutants (A) RJL1 and (B) IAI1. Reverse Primer products were aligned in reverse complement.

A J2315/RJL1

```
PaaI region J2315 (864) ACTGGAGACATGCGGGTCGCTCGCCACCTGTACGTCGCCCAACGGCG
         P166     (194) ACTGGAGTCTAGAGGT---------ACCTGTACGTCGCCCAACGGCG
         P167 rc  (280) ACTGGAGTCTAGAGGT---------ACCTGTACGTCGCCCAACGGCG
         P242     (479) ACTGGAGTCTAGAGGT---------ACCTGTACGTCGCCCAACGGCG
         P243 rc  (501) ------------------------------------------------
       Consensus  (864) ACTGGAGTCTAGAGGT         ACCTGTACGTCGCCCAACGGCG
```

B J2315/IAI1

```
PaaI region J2315 (545) ACTGGAGACATGCGGGTCGCTCGCCACCTGTACGTCGCCCAACGGCG
          P166    (191) ACTGGAGTCTAGAGGT---------ACCTGTACGTCGCCCAACGGCG
          P167 rc (303) ACTGGAGTCTAGAGGT---------ACCTGTACGTCGCCCAACGGCG
          P242    (467) ACTGGAGTCTAGAGGT---------ACCTGTACGTCGCCCAACGGCG
          P243 rc (503) ------------------------------------------------
        Consensus (545) ACTGGAGTCTAGAGGT         ACCTGTACGTCGCCCAACGGCG
```

5 Discsussion

5.1 PaaK1 is not essential for PA degradation in B. cenocepacia

The goal of this work was to characterize two phenylacetyl CoA ligases PaaK1 and PaaK2 in *B. cenocepacia* and in so doing functionally differentiate the two. The results of the *E. coli/B. cenocepacia paaK* complementation indicate that each PA-CoA ligase is fully functional and independent of the other. Additionally, it suggests that PaaK2 complements better with *E. coli* W than PaaK1. However, as PaaK2 was codon optimized to ensure that it would be expressed in *E. coli*, a proper comparison between the two would involve cloning the PaaK2 from the wild type genome, onto the plasmid backbone. Nevertheless, the data demonstrates that both *B. cenocepacia* PA-CoA ligases function and complement in *E. coli W.* This explains why previous insertional mutagenesis of *paaK1* in *B. cenocepacia* resulted in a wild type phenotype (Law et al., 2008). Although our attempt at constructing a *paaK2* and double mutant was unsuccessful, we were able to confirm this for the *B. cenocepacia paaK2* by creating a *paaK1* deletion mutant which grows in PA to slightly higher than wild type levels. Altogether, these results support previous findings that in the absence of a functional PaaK1, *B. cenocepacia* can still grow on PA as a sole carbon source and this is due to the presence of a second functional PA-CoA ligase PaaK2 (Law et al., 2008).

5.2 PaaK1 does not play a direct role in pathogenicity

An initial premise for the hypothesis was that deleting paaK1 would result in an attenuated pathogenicity, as was observed in *paaK1* deletion mutant RJL1. However, complementing *paaK1* back into RJL1 did not restore pathogenicity to wild type levels. The *in vivo* analysis of

the second *paaK1*deletion mutant IAI1 also showed no significant differences in comparison to the wild type strain. The comparative sequence analysis revealed no sequential differences between IAI1 and RJL1 in the region between the two genes flanking *paaK1*. If there is a difference between the two strains, it is likely due to a secondary mutation in the K56-2 wild type strain STC157. Because the *paaK1* insertional mutant also has a wild type-like phenotype, it is reasonable to conclude that the attenuation phenotype observed in RJL1 is not due to a loss of *paaK1*. As such, it stands to reason that PaaK1 is not needed for and may not be involved in the expression of virulence in *B. cenocepacia*.

5.3 PaaK1 function may have to do with substrate variety in the PA pathway

Despite the difficulties that prevented the creation of PaaK2 deletion mutant, we were able to highlight some metabolic differences based on crystallographic reports done on the two PA-CoA ligases by Law and Boulanger which show PaaK1 having a larger more accommodating pocket than PaaK2 . This premise that PaaK1, the activating enzyme of the PA pathway, can also bind 3-OHPA and 4-OHPA (Law and Boulanger, 2011) suggests that these phenolic acids may also be involved in inducing the pathway; particularly 3-OHPA which binds PaaK1 with a lower K_m than 4-OHPA. We supported this finding with the results from our reporter activity assays showing PA pathway induction in minimal media containing 3-OHPA. Phylogenetic analysis of PaaK1 implicates the protein as the native PA-CoA ligase(Law, 2009). In addition to structural considerations, this could account for PaaK1 being more accommodating to larger PA hydroxyl-derivatives.

5.4 3-OHPA induces the PA pathway

Burkholderia cepacia is able to utilize 3-OHPA and 4-OHPA as sole carbon sources (Figure 12) (Arias-Barrau et al., 2004; Méndez et al., 2011).The premise that PaaK1, the activating enzyme of the PA pathway, can also bind 3-OHPA and 4-OHPA (Law and Boulanger, 2011) suggests that these phenolic acids may also be involved in inducing the pathway; particularly 3-OHPA which binds PaaK1 with a lower K_m than 4-OHPA. This assertion was supported with the results from reporter activity assays showing PA pathway induction in minimal media containing 3-OHPA. Our results show that 3-OHPA induces the PA degradative pathway whereas 4-OHPA does not and that this induction is dependent on the presence of a functional *paaK1* gene. As such, they provide support to a differential functional characterization of the phenylacetyl-CoA ligases in *Burkholderia cenocepacia* by showing that although 3-OHPA does bind to PaaK2 (albeit with a lower affinity than *paaK1*) it does not induce the pathway thereafter and is likely not a biological substrate for PaaK2.

The basis of this study was preliminary data showing that a deletion of the *paaK1* gene in *B. cenocepacia* RJL1 resulted in an attenuated killing phenotype in the nematode host model (Law, 2009). According to this finding, Law and Boulanger suggested that the more active, and substrate-versatile PaaK1 might be more beneficial during infection (Law and Boulanger, 2011). However, our results show that PaaK1 (and possibly 3-OHPA) does not play a significant role in pathogenicity. Further work in this area could include an analysis of the intermediates involved in the degradation of 3-OHPA via the PA degradation pathway as well as an investigation of a possible role for PaaK2 in pathogenicity.

5.5 Possible Co-regulation with PaaI

Of particularly note, is the observation that the strain harboring reporter plasmid (pJH6), featuring the *paaZ* promoter, displays double the strength of induction in 3-OHPA than in PA unlike the other two reporter plasmids (pJH7 and pJH8), which register only slightly stronger induction in PA. This is noteworthy because *paaK1* is downstream of, and under the control of the *paaZ* promoter. More interestingly, the next gene upstream of *paaK1* is the *paaI* gene, which encodes a hotdog thioesterase PaaI that preferentially binds 3-OHPA-CoA and 4-OHPA-CoA as substrates compared to PA-CoA (Song et al., 2006). The plot thickens when one considers that PaaI catalyzes the reverse reaction by removing the CoA from PA-CoA. This raises the question of a possible co-regulation of PaaK1 and PaaI. Even as a definitive link has not been made and the specific role of PaaI in the *B. cenocepacia* PA degradative pathway has not been elucidated, we can still speculate that there might be a stronger specific induction of the *paaZ* promoter upon the introduction of 3-OHPA. This induction would require activation of 3-OHPA to 3-OHPA-CoA. Basal levels of expressed PaaK1 would be necessary to allow the pathway to proceed.

5.6 The question of the Paak2 and Double PaaK mutant

A conclusive examination of the role of the PA-CoA ligase will undoubtedly include experiments done with a *paaK2* deletion mutant and a double deletion mutant. We expect that a *paaK2* deletion mutant will also likely grow in PA and 3-OHPA whereas a double deletion mutant will likely produce a PA growth defective mutant and will provide more information about functional differences between the PaaK1 and PaaK2. Because the PaaK1 defective mutant has a wild type-like killing phenotype, it can be speculated that linking the PaaK to pathogenicity

in *B. cenocepacia* will come down to making the link to PaaK2. It is likely that a PaaK2 mutant (and a double mutant) would have an attenuated killing phenotype as would a double mutant.

6 Conclusion

The PA degradative pathway is a central aromatic catabolic pathway that has been demonstrated to be interlinked with pathogenicity (virulence) in *Burkholderia cenocepacia*. In this work, we elaborate on the roles of the two phenylacetyl-CoA ligases PaaK1 and PaaK2 found in *B. cenocepacia* for this pathway by functionally differentiating them based on pathogenicity as well as substrate preference and utilization. In the absence of PaaK1, pathogenicity is not attenuated and remains at wild type levels. Ultimately, loss of function of both genes will be needed to reveal the extent of the involvement of PaaK in pathogenesis.
In addition to the above determination, our results support the findings that PaaK1 is able to bind larger substituted PA compounds such as 3-OHPA by demonstrating that this compound is capable of induction of the PA pathway; and that this induction occurs only in the presence of a functional PaaK1. Besides partially satisfying our stated main objective of functionally differentiating PaaK1 and PaaK2, these results also indicate a possible substrate variability for the PA pathway.

Further work in this area would involve the creation of a *paaK2* deletion mutant and a double *paaK* deletion mutant and assessing the growth of these mutants in PA and their pathogenicity in the nematode host model. Additionally, it would be interesting to ascertain the role 3OHPA plays in PA pathway induction and the biochemical means by which this process occurs as well as a rationale as to why PaaK1 binds 4OHPA or Paak2 binds 3OHPA without apparently inducing the PA degradative pathway.

Bibliography

Aballay, A., and Ausubel, F. M. (2002). *Caenorhabditis elegans* as a host for the study of host-pathogen interactions. *Curr. Opin. Microbiol.* 5, 97-101.

Arias-Barrau, E., Olivera, E. R., Luengo, J. M., Fernandez, C., Galan, B., Garcia, J. L., Diaz, E., and Minambres, B. (2004). The homogentisate pathway: a central catabolic pathway involved in the degradation of L-phenylalanine, L-tyrosine, and 3-hydroxyphenylacetate in *Pseudomonas putida*. *J. Bacteriol.* 186, 5062-5077.

Aubert, D. F., Flannagan, R. S., and Valvano, M. A. (2008). A novel sensor kinase-response regulator hybrid controls biofilm formation and type VI secretion system activity in *Burkholderia cenocepacia*. *Infect. Immun.* 76, 1979-1991.

Balandreau, J., Viallard, V., Cournoyer, B., Coenye, T., Laevens, S., and Vandamme, P. (2001). *Burkholderia cepacia* Genomovar III Is a Common Plant-Associated Bacterium. *Appl. Environ. Microbiol.* 67, 982-985.

Baldwin, A., Sokol, P. A., Parkhill, J., and Mahenthiralingam, E. (2004). The *Burkholderia cepacia* epidemic strain marker is part of a novel genomic island encoding both virulence and metabolism-associated genes in *Burkholderia cenocepacia*. *Infect. Immun.* 72, 1537-1547.

Bazzini, S., Udine, C., Sass, A., Pasca, M. R., Longo, F., Emiliani, G., Fondi, M., Perrin, E., Decorosi, F., Viti, C., Giovannetti, L., Leoni, L., Fani, R., Riccardi, G., Mahenthiralingam, E., and Buroni, S. (2011). Deciphering the Role of RND Efflux Transporters in *Burkholderia cenocepacia*. *PLoS One* 6, e18902.

Burkholder, W. H. (1950). Sour skin, a bacterial rot of onion bulbs. *Phytopathol.* 40, 115-117.

Cao, B., Nagarajan, K., and and Loh, K. C. (2009). Biodegradation of aromatic compounds: current status and opportunities for biomolecular approaches. *Appl Microbiol Biotechnol.* 85, 207-228.

Cardona, S. T., Wopperer, J., Eberl, L., and Valvano, M. A. (2005). Diverse pathogenicity of *Burkholderia cepacia* complex strains in the *Caenorhabditis elegans* host model. *FEMS Microbiol. Lett.* 250, 97-104.

Cohen, S. N., Chang, A. C., and Hsu, L. (1972). Nonchromosomal antibiotic resistance in bacteria: Genetic transformation of *Escherichia coli* by R-factor DNA. *Proc. Natl. Acad. Sci. U. S. A.* 69, 2110-2114.

Compant, S., Nowak, J., Coenye, T., Clément, C., and Ait Barka, E. (2008). Diversity and occurrence of Burkholderia spp. in the natural environment. *FEMS Microbiol Rev.* 4, 607-626.

Copley, S. D. (1997). Diverse mechanistic approaches to difficult chemical transformations: microbial dehalogenation of chlorinated aromatic compoun. *Chem Biol.* 4, 169-74.

Craig, F. F., Coote, J. G., Parton, R., Freer, J. H., and Gilmour, N. J. (1989). A plasmid which can be transferred between *Escherichia coli* and *Pasteurella haemolytica* by electroporation and conjugation. *J. Gen. Microbiol.* 135, 2885-2890.

Darling, P., Chan, M., Cox, A. D., and Sokol, P. A. (1998). Siderophore production by cystic fibrosis isolates of *Burkholderia cepacia*. *Infect. Immun.* 66, 874-877.

del Peso-Santos, T., Shingler, V., and Perera, J. (2008). The styrene-responsive StyS/StyR regulation system controls expression of an auxiliary phenylacetyl-coenzyme A ligase: implications for rapid metabolic coupling of the styrene upper- and lower-degradative pathways. *Mol. Microbiol.* 69, 317-330.

Díaz, E. (2004). Bacterial degradation of aromatic pollutants: a paradigm of metabolic versatility. *Int Microbiol.* 7, 173-180.

Diaz, E., Ferrandez, A., Prieto, M. A., and Garcia, J. L. (2001). Biodegradation of aromatic compounds by *Escherichia coli*. *Microbiol. Mol. Biol. Rev.* 65, 523-569.

Drevinek, P., and Mahenthiralingam, E. (2010). *Burkholderia cenocepacia* in cystic fibrosis: epidemiology and molecular mechanisms of virulence. *Clin. Microbiol. Infect.* 16, 821-830.

Dubarry, N., Du, W., Lane, D., and Pasta, F. (2010). Improved electrotransformation and decreased antibiotic resistance of the cystic fibrosis pathogen Burkholderia cenocepacia strain J2315. *Appl. Environ. Microbiol.* 76, 1095-1102.

El-Said Mohamed, M. (2000). Biochemical and molecular characterization of phenylacetate-coenzyme A ligase, an enzyme catalyzing the first step in aerobic metabolism of phenylacetic acid in *Azoarcus evansii*. *J. Bacteriol.* 182, 286-294.

Ferrandez, A., Minambres, B., Garcia, B., Olivera, E. R., Luengo, J. M., Garcia, J. L., and Diaz, E. (1998). Catabolism of phenylacetic acid in *Escherichia coli*. Characterization of a new aerobic hybrid pathway. *J. Biol. Chem.* 273, 25974-25986.

Field, J. A., and Sierra-Alvarez, R. (2008). Microbial transformation and degradation of polychlorinated biphenyls. *Environmental Pollution* 155, 1-12.

Figurski, D. H., and Helinski, D. R. (1979). Replication of an origin-containing derivative of plasmid RK2 dependent on a plasmid function provided in trans. *Proc. Natl. Acad. Sci. U. S. A.* 76, 1648-1652.

Flannagan, R. S., Linn, T., and Valvano, M. A. (2008). A system for the construction of targeted unmarked gene deletions in the genus *Burkholderia*. *Environ. Microbiol.* 10, 1652-1660.

Garcia, B., Olivera, E. R., Minambres, B., Carnicero, D., Muniz, C., Naharro, G., and Luengo, J. M. (2000). Phenylacetyl-coenzyme A is the true inducer of the phenylacetic acid catabolism pathway in *Pseudomonas putida* U. *Appl. Environ. Microbiol.* 66, 4575-4578.

Goris, J., De Vos, P., Caballero-Mellado, J., Park , J., Falsen, E., Quensen, J. F. 3., Tiedje, J. M., and Vandamme, P. (2004). Classification of the biphenyl- and polychlorinated biphenyl-degrading strain LB400T and relatives as Burkholderia xenovorans sp. nov. *Int J Syst Evol Microbiol.* 54, 1677-1681.

Gulick, A. M. (2009). Conformational Dynamics in the Acyl-CoA Synthetases, Adenylation Domains of Non-Ribosomal Peptide Synthetases, and Firefly Luciferase. *ACS Chem Biol.* 4, 811-827.

Gulick, A. M., Lu, X., and Dunaway-Mariano, D. (2004). Crystal structure of 4-chlorobenzoate:CoA ligase/synthetase in the unliganded and aryl substrate-bound states. *Biochemistry* 43, 8670-8679.

Hamlin, J. N., Bloodworth, R. A., and Cardona, S. T. (2009). Regulation of phenylacetic acid degradation genes of *Burkholderia cenocepacia* K56-2. *BMC Microbiol.* 9, 222.

Holden, M. T., Seth-Smith, H. M., Crossman, L. C., Sebaihia, M., Bentley, S. D., Cerdeno-Tarraga, A. M., Thomson, N. R., Bason, N., Quail, M. A., Sharp, S., Cherevach, I., Churcher, C., Goodhead, I., Hauser, H., Holroyd, N., Mungall, K., Scott, P., Walker, D., White, B., Rose, H., Iversen, P., Mil-Homens, D., Rocha, E. P., Fialho, A. M., Baldwin,

A., Dowson, C., Barrell, B. G., Govan, J. R., Vandamme, P., Hart, C. A., Mahenthiralingam, E., and Parkhill, J. (2009). The genome of *Burkholderia cenocepacia* J2315, an epidemic pathogen of cystic fibrosis patients. *J. Bacteriol.* 191, 261-277.

Hunt, T. A., Kooi, C., Sokol, P. A., and Valvano, M. A. (2004). Identification of *Burkholderia cenocepacia* genes required for bacterial survival in vivo. *Infect. Immun.* 72, 4010-4022.

Imolorhe, I. A., and and Cardona, S. T. (2011). 3-Hydroxyphenylacetic acid induces the Burkholderia cenocepacia phenylacetic acid degradation pathway – toward understanding the contribution of aromatic catabolism to pathogenesis. *Front. Cell. Inf. Microbio.* 1, 14-7.

Isles, A., Maclusky, I., Corey, M., Gold, R., Prober, C., Fleming, P., and Levison, H. (1984). *Pseudomonas cepacia* infection in cystic fibrosis: an emerging problem. *J. Pediatr.* 104, 206-210.

Izard, N. C., Hächler, H., Grehn, M., and Kayser, F. H. (1992). Ribotyping of Coagulase-Negative Staphylococci with Special Emphasis on Intraspecific Typing of *Staphylococcus epidermidis* . *ASM* Vol. 30, No. 4, 817-823.

Kooi, C., and Sokol, P. A. (2009). Burkholderia cenocepacia zinc metalloproteases influence resistance to antimicrobial peptides. *Microbiology* 155, 2818-25-2825.

Kothe, M., Antl, M., Huber, B., Stoecker, K., Ebrecht, D., Steinmetz, I., and Eberl, L. (2003). Killing of *Caenorhabditis elegans* by *Burkholderia cepacia* is controlled by the cep quorum-sensing system. *Cell. Microbiol.* 5, 343-351.

Kurz, C. L., and Ewbank, J. J. (2003). Caenorhabditis elegans: an emerging genetic model for the study of innate immunity. *Nat. Rev. Genet.* 4, 380-390.

Law, A., and Boulanger, M. J. (2011). Defining a Structural and Kinetic Rationale for Paralogous Copies of Phenylacetate-CoA Ligases from the Cystic Fibrosis Pathogen *Burkholderia cenocepacia* J2315. *J. Biol. Chem.* 286, 15577-15585.

Law, R. J. (2009). The Relationship between Phenylacetic acid Catabolism and Pathogenicity of *Burkholderia cenocepacia* K56-2 in the *Caenorhabditis elegans* Host Model.

Law, R. J., Hamlin, J. N. R., Sivro, A., McCorrister, S. J., Cardama, G. A., and Cardona, S. T. (2008). A functional phenylacetic acid catabolic pathway is required for full pathogenicity of *Burkholderia cenocepacia* in the *Caenorhabditis elegans* host model. *J. Bacteriol.* 190, 7209-7218.

Lim, Y. W., Baik, K. S., Han, S. K., Kim, S. B., and Bae, K. S. (2003). *Burkholderia sordidicola* sp. nov., isolated from the white-rot fungus *Phanerochaete sordida*. *Int J Syst Evol Microbiol.* 5, 1631-1636.

Loutet, S. A., and Valvano, M. A. (2010). A decade of *Burkholderia cenocepacia* virulence determinant research. *Infect. Immun.* 78, 4088-4100.

Lu, X. Y., Zhang, T., and and Han-Ping Fang, H. (2011). Bacteria-mediated PAH degradation in soil and sediment. *Appl Microbiol Biotechnol.* 5, 1357-1371.

Luengo, J. M., Garcia, J. L., and Olivera, E. R. (2001). The phenylacetyl-CoA catabolon: a complex catabolic unit with broad biotechnological applications. *Mol. Microbiol.* 39, 1434-1442.

Mahenthiralingam, E., Baldwin, A., and Dowson, C. G. (2008). *Burkholderia cepacia* complex bacteria: opportunistic pathogens with important natural biology. *J. Appl. Microbiol.* 104, 1539.

Malott, R. J., O'Grady, E. P., Toller, J., Inhulsen, S., Eberl, L., and Sokol, P. A. (2009). A Burkholderia cenocepacia orphan LuxR homolog is involved in quorum-sensing regulation. *J. Bacteriol.* 191, 2447-2460.

Martinez-Blanco, H., Reglero, A., and Luengo, J. M. (1990a). Carbon catabolite regulation of phenylacetyl-CoA ligase from *Pseudomonas putida* . *Biochem. Biophys. Res. Commun.* 167, 891-897.

Martinez-Blanco, H., Reglero, A., Rodriguez-Aparicio, L. B., and Luengo, J. M. (1990b). Purification and biochemical characterization of phenylacetyl-CoA ligase from *Pseudomonas putida*. A specific enzyme for the catabolism of phenylacetic acid. *J. Biol. Chem.* 265, 7084-7090.

Méndez, V., Agulló, L., González, M., and Seeger, M. (2011). The Homogentisate and Homoprotocatechuate Central Pathways Are Involved in 3- and 4-Hydroxyphenylacetate Degradation by *Burkholderia xenovorans* LB400. *PLos ONE* 6, 1-9.

Miller, V. L., and Mekalanos, J. J. (1988). A novel suicide vector and its use in construction of insertion mutations: osmoregulation of outer membrane proteins and virulence determinants in *Vibrio cholerae* requires toxR. *J. Bacteriol.* 170, 2575-2583.

Miñambres, B., Martínez-Blanco, H., Olivera, E. R., García, B., Díez, B., Barredo, J. L., Moreno, M. A., Schleissner, C., Salto, F., and Luengo, J. M. (1996). Molecular cloning and expression in different microbes of the DNA encoding Pseudomonas putida U phenylacetyl-CoA ligase. Use of this gene to improve the rate of benzylpenicillin biosynthesis in Penicillium chrysogenum. *J Biol Chem.* 271, 33531-33538.

Mingot, J. M., Penalva, M. A., and Fernandez-Canon, J. M. (1999). Disruption of phacA, an *Aspergillus nidulans* gene encoding a novel cytochrome P450 monooxygenase catalyzing phenylacetate 2-hydroxylation, results in penicillin overproduction. *J. Biol. Chem.* 274, 14545-14550.

O'Sullivan, B. P., and Freedman, S. D. (2009). Cystic Fibrosis. *Lancet* Vol 373, 1891-1904.

Peeters, E., Nelis, H. J., and Coenye, T. (2008). Resistance of planktonic and biofilm-grown Burkholderia cepacia complex isolates to the transition metal gallium. *Journal of Antimicrobial Chemotherapy* 61, 1062-1065.

Quinton, P. M. (2008). Cystic fibrosis: impaired bicarbonate secretion and mucoviscidosis. *Lanclet* 372, 415-417.

Ramos, C. G., Sousa, S. A., Grilo, A. M., Eberl, L., and Leitão, J. H. (2010). The Burkholderia cenocepacia K56-2 pleiotropic regulator Pbr, is required for stress resistance and virulence. *Microb Pathog.* 48, 168-177.

Rodriguez-Saiz M, Barredo JL, Moreno MA, J.M., Fernandez-Canon JM, Penalva MA, and Diez B. (2001). Reduced function of a phenylacetate-oxidizing cytochrome p450 caused strong genetic improvement in early phylogeny of penicillin-producing strains. *J Bacteriol.2001 Oct;183(19):5465-71.*

Saldias, M. S., and Valvano, M. A. (2009). Interactions of *Burkholderia cenocepacia* and other *Burkholderia cepacia* complex bacteria with epithelial and phagocytic cells. *Microbiology* 155, 2809-2817.

Santos, A. V., Dillon, R. J., Dillon, V. M., Reynolds, S. E., and Samuels, R. I. (2004). Ocurrence of the antibiotic producing bacterium Burkholderia sp. in colonies of the leaf-cutting ant Atta sexdens rubropilosa. *FEMS Microbiol Lett.* 2, 319-323.

Schmelz, S., and Naismith, J. H. (2009). Adenylate-forming enzymes. *Curr Opin Struct Biol.* 6, 666-671.

Song, F., Zhuang, Z., Finci, L., Dunaway-Mariano, D., Kniewel, R., Buglino, J. A., Solorzano, V., Wu, J., and Lima, C. D. (2006). Structure, function, and mechanism of the phenylacetate pathway hot dog-fold thioesterase PaaI. *J. Biol. Chem.* 281, 11028-11038.

Sousa, S. A., Ramos, C. G., and Leitao, J. H. (2011). *Burkholderia cepacia* Complex: Emerging Multihost Pathogens Equipped with a Wide Range of Virulence Factors and Determinants. *Int. J. Microbiol.* 2011, 607575. Epub 2010 Aug 3.

Stiernagle, T. (1999). "Maintenance of *C. elegans*," in ***C. elegans: A Practical Approach,*** ed., I. A. Hope Oxford University Press), 51-67.

Teufel, R., Gantert, C., Voss, M., Eisenreich, W., Haehnel, W., and Fuchs, G. (2011). Studies on the mechanism of ring hydrolysis in phenylacetate degradation: a metabolic branching point. *J. Biol. Chem.* 286, 11021-11034.

Teufel, R., Mascaraque, V., Ismail, W., Voss, M., Perera, J., Eisenreich, W., Haehnel, W., and Fuchs, G. (2010). Bacterial phenylalanine and phenylacetate catabolic pathway revealed. *Proc. Natl. Acad. Sci. U. S. A.* 107, 14390-14395.

Tomich M, FAU - Herfst, C. A., Herfst CA, FAU - Golden, J. W., Golden JW, FAU - Mohr, C. D., and Mohr CD. (2002). Role of flagella in host cell invasion by Burkholderia cepacia. *Infect Immun.* 4, 1799-1806.

Tomlin, K. L., Coll, O. P., and Ceri, H. (2001). Interspecies biofilms of *Pseudomonas aeruginosa* and *Burkholderia cepacia*. *Can J Microbiol.* 47, 949-954.

Urban TA, FAU - Griffith, A., Griffith A, FAU - Torok, A. M., Torok AM, FAU - Smolkin, M. E., Smolkin ME, FAU - Burns, J. L., Burns JL, FAU - Goldberg, J. B., and Goldberg

JB. (2004). Contribution of Burkholderia cenocepacia flagella to infectivity and inflammation. *Infect Immun.2004 Sep;72(9):5126-34.*

Urban, T. A., Goldberg, J. B., Forstner, J. F., and Sajjan, U. S. (2005). Cable pili and the 22-kilodalton adhesin are required for Burkholderia cenocepacia binding to and transmigration across the squamous epithelium. *Infect Immun.* 73, 5426-5437.

Valvano, M. A., Keith, K. E., and Cardona, S. T. (2005). Survival and persistence of opportunistic *Burkholderia* species in host cells. *Curr. Opin. Microbiol.* 8, 99-105.

Vandamme, P., Holmes, B., Vancanneyt, M., Coenye, T., Hoste, B., Coopman, R., Revets, H., Lauwers, S., Gillis, M., Kersters, K., and Govan, J. R. (1997). Occurrence of multiple genomovars of *Burkholderia cepacia* in cystic fibrosis patients and proposal of *Burkholderia multivorans* sp. nov. *Int. J. Syst. Bacteriol.* 47, 1188-1200.

Villemur, R. (1995). Coenzyme A ligases involved in anaerobic biodegradation of aromatic compounds. *Can J Microbiol.* 41, 855-861.

Vitovski, S. (1993). Phenylacetate-coenzyme A ligase is induced during growth on phenylacetic acid in different bacteria of several genera. *FEMS Microbiol Lett.* 108, 1-5.

Yabuuchi, E., Kosako, Y., Oyaizu, H., Yano, I., Hotta, H., Hashimoto, Y., Ezaki, T., and Arakawa, M. (1992). Proposal of *Burkholderia* gen. nov. and transfer of seven species of the genus *Pseudomonas* homology group II to the new genus, with the type species *Burkholderia cepacia* (Palleroni and Holmes 1981) comb. nov. *Microbiol. Immunol.* 36, 1251-1275.

Yudistira, H., McClarty, L., Bloodworth, R. A., Hammond, S. A., Butcher, H., Mark, B. L., and Cardona, S. T. (2011). Phenylalanine induces *Burkholderia cenocepacia* phenylacetic

acid catabolism through degradation to phenylacetyl-CoA in synthetic cystic fibrosis sputum medium. *Microb. Pathog.* 51, 183-196.

Zhang, C., and Bennett , G. N. (2005). Biodegradation of xenobiotics by anaerobic bacteria. *Appl Microbiol Biotechnol* 67, 600-618.